

# Bayesian inference for stochastic differential equation mixed effects models of a tumor xenography study

Umberto Picchini<sup>a</sup>, Julie Lyng Forman<sup>b</sup>

<sup>a</sup>Centre for Mathematical Sciences, Lund University  
Sölvegatan 18, SE-22100 Lund, Sweden  
Email: [umberto@maths.lth.se](mailto:umberto@maths.lth.se)

<sup>b</sup>Section of Biostatistics, Department of Public Health, University of Copenhagen  
Øster Farimagsgade 5, DK-1014 Copenhagen K, Denmark  
Email: [juf@biostat.ku.dk](mailto:juf@biostat.ku.dk)

## Abstract

We model the growth dynamics of repeated measurements of tumor volumes in mice. We consider a two compartments representation corresponding to the fractions of tumor cells killed by and survived to a treatment, respectively. Dynamics are modelled with stochastic differential equations, resulting in new state-space stochastic differential equation mixed effects models (SDEMEM) for response to treatment and regrowth. We considered Bayesian inference for model parameters, using both exact methodology based on sequential Monte Carlo and an approximate one using synthetic likelihoods. A case study considers data from a tumor xenography study with two treatment groups and one control, each containing 5-8 mice. Results from the case study and from a simulation study show that our models are able to reproduce the observed growth patterns and that Bayesian synthetic likelihoods perform similarly to exact Bayesian inference. This opens up possibilities to study SDEMEMs that are not restricted to state-space models. With the small sample sizes as in the case study, prior information is needed to identify all model parameters, while in simulations with a larger sample of 17 mice per group unidentifiability is no longer an issue.

**Keywords:** intractable likelihood; repeated measurements; particle MCMC; state-space model; synthetic likelihood.

## 1 Introduction

Pre-clinical cancer trials aim at understanding the dynamics of tumor growth and evaluate the effect of treatments such as radio- and chemotherapies in delaying this. A typical trial involves repeated measurements of the volume of solid tumors grown in mice. Tumors are grown until a critical size is reached, in case of which the mouse must be sacrificed for ethical reasons, or until a planned end of study. Data from these trials pose a statistical challenge due to the missing data caused by the sacrifice and due to the substantial variation in growth patterns between subjects. Even within the same treatment group, it occurs that some tumors are eliminated following treatment, others continue to grow unaffected, and yet others display a decrease in volume followed by regrowth [Laajala et al., 2012].

Heitjan et al. [1993] review traditional approaches to analysing tumor xenography experiments, including ANOVA, MANOVA, and linear mixed models for tumor volumes. An overall drawback of linear models is that inference targets the mean log-volume of the tumor. This is problematic, since tumor volumes are very often censored due to ethical guidelines that prohibit large size tumors from ever being observed. An alternative comparison of two treatments can be obtained from a log-rank test on the time to sacrifice, tumor doubling times, or similar survival

outcomes. Other approaches to analyzing tumor growth, which rely on methods from survival analysis, include models of tumor delay and log cell kill (inferred from tumor quadrupling times), see [Stuschke et al. \[1990\]](#), [Wu and Houghton \[2009\]](#) and [Wu \[2011\]](#). However, these approaches have limited efficiency as they do not make use of the full information in the data. Moreover, delays and doubling times may in practice be hard to measure accurately due to day-to-day perturbations in growth, measurement error, and discrete time follow-up. Rank-based comparisons of composite tumor volume/time to sacrifice outcomes [[Péron et al., 2016](#)] is a more robust and powerful approach. However, it does not offer much insight on the tumor growth dynamics and effect of the treatment. Also a fully specified parametric model would be required for power calculations and optimal design.

[Demidenko \[2013\]](#) reviews non-linear mixed models for tumor growth including the exponential, double exponential and delayed double exponential model for re-growth following treatment. We will focus on the double exponential model which identifies two latent compartments corresponding to the fraction of the tumor which is killed by the treatment and the one that survives. This model offers a phenomenological explanation for the variation in individual tumor growth patterns, by recognizing a) the proportion of the tumor killed by the treatment, b) the rate of elimination of the dead tumor cells, and c) the growth rate of the surviving part of the tumor. Clinically relevant quantities such as tumor doubling times, tumor growth delay and surviving fraction of tumor cells can be deduced from the double exponential model, as shown in [Demidenko \[2006\]](#) and [Demidenko \[2010\]](#). More recent non-linear mixed model approaches specify the individual growth curves semi-parametrically [[Xia et al., 2013](#)], or as splines ([Kong and Yan, 2011](#), [Zhao et al., 2011](#)). These models allow for much flexibility in individual growth curves but do not share the biological interpretation of the double exponential or delayed double exponential models. A drawback of the double exponential, and other classical non-linear mixed models, is that the only source of intra-subject variation is given by independent identically distributed measurement errors. This is not realistic as growth rates are subject to day-to-day variation, due to biological processes not easily accounted for.

In recent years, a number of works have promoted the use of stochastic differential equation mixed effects models (SDEMEmS) as a more realistic alternative to the classical nonlinear mixed models. For instance, [Donnet et al. \[2010\]](#) find that a stochastic differential equation version of the Gompertz growth model is superior to its nonlinear deterministic mixed model counterpart, for prediction of the body weight of growing chicken. [Donnet and Samson \[2013\]](#) report similar findings from pharmacokinetic experiments. Recent contributions to SDEMEmS inference are [Delattre and Lavielle \[2013\]](#) and [Whitaker et al. \[2016\]](#), see in particular the latter for an account of recent contributions. In general, even when not considering experiments involving repeated experiments, inference for stochastic differential equations (SDEs) is challenging [[Fuchs, 2013](#)], because nonlinear SDE models have unknown transition densities, hence intractable likelihood functions. An additional difficulty is that we do not assume availability of measurements from a Markov process (solution to an SDE), instead we consider observations to be affected by measurement noise. Hence the class of models we formulate in this paper is of state-space type (hidden Markov models, [Cappé et al., 2006](#)). It is possible to treat state-space models, including those having dynamics given by an SDE, using state-of-art likelihood-based methods based on sequential Monte Carlo (SMC) filters. Indeed, in one of our attempts at estimating model parameters, we use a particle marginal method [[Andrieu and Roberts, 2009](#)] which returns exact Bayesian inference, despite employing SMC approximations. However we also consider a methodology which is able to target more general models, beyond the state space class: we use a Bayesian version of the synthetic likelihoods (SL) approach due to [Price et al. \[2017\]](#). SL was initially proposed in [Wood \[2010\]](#) and does not impose any assumption on the complexity of the model, the only requirement being the ability to simulate artificial datasets from the model and construct summary statistics for the generated datasets. We show that using Bayesian SL (BSL) with SDEMEmS produces results qualitatively similar to the exact

Bayesian methodology, both with real experimental data and with artificial data produced in a simulation study. Also, we find that BSL is able to identify model parameters correctly and distinguish different treatment efficacies in a simulation study with seventeen subjects in each treatment group. When considering application to experimental data, we find that having only 5-8 subjects per treatment group is not enough to identify all model parameters accurately. Nevertheless, Bayesian inference still offers an opportunity to perform exploratory data analyses in small scale experiments, since informative priors based on subject matter expertise may compensate for otherwise too small sample sizes.

Although SDEMEmS are complex models with three layers of randomness, as described in next sections, we conclude that BSL can be considered as an additional tool for inference in this class of models. Most importantly, in future studies we could redefine the model to be of non-state-space type, and in such scenario exact parameter inference via sequential Monte Carlo (particle) methods might not be an option, while BSL can still be applied.

The structure of the paper is as follows: Section 2 contrasts the classical nonlinear mixed models with the stochastic differential equation mixed effects models (SDEMEmS). Section 3 considers a particle marginal method for exact Bayesian inference in SDEMEmS. Section 4 considers the approach using synthetic likelihoods. To the best of our knowledge this is the first application of synthetic likelihoods to SDEMEmS. In section 5 we analyse data from a tumor xenography study including two treatment groups and a control, each containing 5-8 mice. Results indicate that the suggested models are appropriate for describing tumor growth and response to treatment, but some model parameters are poorly identified due to the small sample size. Finally, in section 6 we run two simulation studies on artificial data.

## 2 Mixed effects models of tumor growth

### 2.1 Ordinary mixed effects models

Denote with  $M$  the number of subjects in a given treatment group. Assume that tumor volumes from subject  $i$  are measured at discrete time points  $t_{i0} < \dots < t_{in_i}$ ,  $i = 1, \dots, M$ . In a planned experiment, such as the one considered in section 5, time points will usually be the same for all subjects, i.e.  $t_{ij} = t_j$ , but the number of observations  $n_i$  may differ between subjects. For instance, the mice in the above mentioned experiment were sacrificed when their tumor volume exceeded a critical size prescribed by the ethical guidelines. Denote with  $V_{ij} = V_i(t_j)$  the exact tumor volume of subject  $i$  at time  $t_j$ ,  $j = 1, \dots, n_i$ . We model the observations as

$$Y_{ij} = \log(V_{ij}) + \varepsilon_{ij}, \quad i = 1, \dots, M; j = 1, \dots, n_i \quad (1)$$

where the  $\varepsilon_{ij}$ 's are i.i.d. normally distributed measurements errors with  $\varepsilon_{ij} \sim \mathcal{N}(0, \sigma_\varepsilon^2)$ . This means that we assume tumor volumes to be measured with multiplicative log-normal measurement errors. Experimental practice consists in measuring the length and width of the tumor and approximate its volume by that of an ellipsoid, which results in a measurement accuracy that is typically within  $\pm 20\%$  of the true volume.

In regulated experiments the mice are sacrificed long before the tumor volumes reach steady state. Hence, unperturbed growth in the control group is adequately described by a simple exponential growth model. Let  $\beta_1, \dots, \beta_M$  denote the random subject-specific growth rates, then the growth curves for the control group are given by

$$\frac{dV_i(t)}{dt} = \beta_i V_i(t), \quad V_i(0) = v_{i,0}, \quad i = 1, \dots, M. \quad (2)$$

Distributional assumptions for the  $\beta_i$ 's are in section 2.2. Of course, equation (2) is solved explicitly by  $V_i(t) = v_{i,0} e^{\beta_i t}$ . Note that with the further assumption that growth rates are normally distributed and initial tumor volumes log-normally distributed across the population,

the observation model (1) is merely a standard linear mixed model with a random intercept and a random slope.

If tumor volumes are observed post treatment, then the double exponential model in [Demidenko \[2013\]](#) describes the total volume in terms of surviving tumor cells  $V^{\text{surv}}$  and cells killed by the treatment  $V^{\text{kill}}$  as

$$\begin{cases} V_i(t) &= V_i^{\text{surv}}(t) + V_i^{\text{kill}}(t), \\ \frac{dV_i^{\text{surv}}(t)}{dt} &= \beta_i V_i^{\text{surv}}(t), \quad V_i^{\text{surv}}(0) = (1 - \alpha_i)v_{i,0}, \quad i = 1, \dots, M \\ \frac{dV_i^{\text{kill}}(t)}{dt} &= -\delta_i V_i^{\text{kill}}(t), \quad V_i^{\text{kill}}(0) = \alpha_i v_{i,0}. \end{cases} \quad (3)$$

Here  $\alpha_i \in [0, 1]$  denotes the proportion of the tumor that has been killed by the treatment in subject  $i$ , while  $\delta_i$  denotes the elimination rate for the dead tumor cells in subject  $i$ . Equation (3) has the explicit solution  $V_i(t) = (1 - \alpha_i)v_{i,0}e^{\beta_i t} + \alpha_i v_{i,0}e^{-\delta_i t}$ . Distributional assumptions for  $\delta_i$  and  $\alpha_i$  are in section 2.2. Note that if tumors were allowed to grow beyond the limit of the ethical guidelines, then the volumes of long-term surviving mice would eventually reach a steady state. In this case data would more adequately be described by growth curves such as the Gompertz, Richards, Weibull or Logistic, see e.g. [Heitjan \[1991\]](#).

## 2.2 Stochastic differential equation mixed effects model

The assumption of time constant growth and elimination rates in the ordinary mixed models is usually not realistic, since growth is affected by various biological processes that are not easily accounted for. [Donnet et al. \[2010\]](#) used a stochastic differential equation (SDE) version of the Gompertz curve to model the body weights of chicken over time. They found that the SDE model provided much more accurate dynamical predictions of individual weights, compared to ordinary differential equation models.

We therefore suggest to replace the ordinary differential equation model specified by (2) with a SDE model such as the geometric Brownian motion,

$$dV_i(t) = (\beta_i + \gamma^2/2)V_i(t)dt + \gamma V_i(t)dB_i(t), \quad V_{i,0} = v_{i,0}. \quad (4)$$

Here the  $\{B_{i,t}\}_{t \geq 0}$ 's are independent standard Brownian motions and  $\gamma^2$  denotes the intra-subject growth rate variance. This means that the instantaneous growth rate is not exactly  $\beta_i$  but deviates from this by a random normal perturbation (white noise). The motivation for including the term  $\gamma^2/2$  in the drift of the SDE is that the individual growth process is then given by  $V_i(t) = v_{i,0}e^{\beta_i t + \gamma B_i(t)}$  which is a log-normally distributed stochastic process with median (geometric mean)  $v_{i,0}e^{\beta_i t}$ , which coincides with the ordinary exponential growth model (2). With the further assumption that growth rates are distributed as  $\beta_i \sim \mathcal{N}(\bar{\beta}_0, \sigma_\beta^2)$  and initial tumor volumes as  $\log(v_{i,0}) \sim \mathcal{N}(\bar{v}_0, \sigma_0^2)$  across the population, volumes at time  $t_{ij}$  would follow a log-normal distribution with median (geometric mean)  $\bar{v}_0 e^{\bar{\beta}_0 t_{ij}}$  which is the same as in the ordinary log-linear mixed model. However, to rule out negative growth rates, we prefer to make the assumption  $\log \beta_i \sim \mathcal{N}(\bar{\beta}, \sigma_\beta)$  when analysing our case study data. Also, we assume  $v_{i0}$  to be fixed known mathematical constants.

The ordinary double exponential model (3) can similarly be replaced by a stochastic differential equation mixed effects model with the following specification

$$\begin{cases} Y_{ij} &= \log(V_{ij}) + \varepsilon_{ij}, \quad i = 1, \dots, M; \quad j = 1, \dots, n_i \\ V_i(t) &= V_i^{\text{surv}}(t) + V_i^{\text{kill}}(t), \\ dV_i^{\text{surv}}(t) &= (\beta_i + \gamma^2/2)V_i^{\text{surv}}(t)dt + \gamma V_i^{\text{surv}}(t)dB_i(t), \quad V_i^{\text{surv}}(0) = (1 - \alpha_i)v_{i,0} \\ dV_i^{\text{kill}}(t) &= (-\delta_i + \tau^2/2)V_i^{\text{kill}}(t)dt + \tau V_i^{\text{kill}}(t)dW_i(t), \quad V_i^{\text{kill}}(0) = \alpha_i v_{i,0} \end{cases} \quad (5)$$

with random effects  $\log \beta_i \sim \mathcal{N}(\bar{\beta}, \sigma_\beta^2)$ ,  $\log \delta_i \sim \mathcal{N}(\bar{\delta}, \sigma_\delta^2)$  and  $\log \alpha_i \sim \mathcal{N}_{[0,1]}(\bar{\alpha}, \sigma_\alpha^2)$  where  $\mathcal{N}_{[0,1]}$  is a Gaussian distribution truncated to the interval  $[0,1]$ . The  $\{W_i(t)\}_{t \geq 0}$ 's are additional standard

Brownian motions assumed mutually independent and independent of the  $\{B_i(t)\}_{t \geq 0}$ 's, of the  $\varepsilon_{ij}$ , of the (fixed) system initial conditions and of the random effects. Here  $\tau^2$  denotes the intra-subject elimination rate variance. The SDEs in (5) have explicit solutions given by  $V_i^{\text{surv}}(t) = V_i^{\text{surv}}(0)e^{\beta_i t + \gamma dB_i(t)}$  and  $V_i^{\text{kill}}(t) = V_i^{\text{kill}}(0)e^{-\delta_i t + \tau dW_i(t)}$  respectively. This means that it is easy to simulate paths from (5): for example for an observational time step  $\Delta_{ij} := t_{ij} - t_{i,j-1}$ , we have that at sampling time  $t_{ij}$  it holds  $V_i^{\text{surv}}(t_{ij}) = V_i^{\text{surv}}(t_{i,j-1})e^{\beta_i \Delta_{ij} + \gamma \Delta_{ij}^{1/2} \xi_{ij}}$  with  $\{\xi_{ij}\}$  independent draws from  $\mathcal{N}(0, 1)$  (and independent of  $\varepsilon_{ij}$  and the random effects), and similarly for  $V_i^{\text{kill}}(t_{ij})$ , so that  $V_{ij} = V_i^{\text{surv}}(t_{ij}) + V_i^{\text{kill}}(t_{ij})$ .

Finally, we point out that models (4) and (5) by no means are the only possible ways of specifying SDEMEmS for tumor growth. Diffusion terms of the type  $\gamma V_i(t) dB_i(t)$  could be replaced by a more flexible form such as  $\gamma V_i(t)^\rho dB_i(t)$  (for some exponent  $\rho$ ). Alternatively a so-called ‘‘stochastic growth rate model’’ could be specified by  $V_i(t) = \exp\{\int_0^t \beta_i(u) du\}$ , where the time-varying growth rate  $\{\beta_i(t)\}_{t \geq 0}$  for instance could be modelled by the Ornstein-Uhlenbeck process  $d\beta_i(t) = -\rho_i(\beta_i(t) - \bar{\beta}_i)dt + \gamma_i dB_i(t)$ , which evolves as a continuous time autoregressive process around its mean  $\bar{\beta}_i$ . These alternative models do not admit simple closed form solutions like (4) and (5) do, but can still be analyzed using the Bayesian methods described in this paper. However, since the integrated diffusion process in the stochastic growth rate model is not a Markov process, the more general methodology from section 4 would be needed to analyze this particular model.

### 3 Likelihood-based inference for SDEMEmS

In this section we discuss likelihood inference for SDEMEmS such as model (4) and (5) and generalizations thereof. Both models can be viewed as instances of the general state-space SDEMEm

$$\begin{cases} Y_{ij} &= g(X_i(t_{ij}), \varepsilon_{ij}), & \varepsilon_{ij} \sim_{i.i.d.} N(0, \sigma_\varepsilon^2) \\ dX_i(t) &= \mu(X_{it}, t, \phi_i)dt + \sigma(X_{it}, t, \kappa)dB_i(t), & X_i(t_0) \sim \pi_0(x_i(t_0)|\phi_i) \\ \phi_i &\sim_{i.i.d.} p(\phi_i|\eta). \end{cases} \quad (6)$$

Model (6) has the following interpretation: for each subject  $i$ ,  $\{X_{it}\}_{t \geq 0}$  represents the hidden (unobservable) biological process of interest, with dynamics governed by the drift and diffusion functions  $\mu(\cdot)$  and  $\sigma(\cdot)$  which are assumed known, save from the the subject specific parameters (random effects)  $\phi_i$  and the common model parameters  $\kappa$ . In case of model (5), the latent process is  $X_i(t) = (V_i^{\text{kill}}, V_i^{\text{surv}})$ ,  $\kappa = (\gamma, \tau)$ ,  $\phi_i = (\log \alpha_i, \log \beta_i, \log \delta_i)$ ,  $\eta = (\bar{\alpha}, \bar{\beta}, \bar{\delta}, \sigma_\alpha, \sigma_\beta, \sigma_\delta)$ . Regularity conditions for the existence and uniqueness of a solution to the stochastic differential equation can be found e.g. in [Fuchs \[2013\]](#). Direct observation of  $\{X_i(t)\}$  is assumed impossible, hence data  $Y_{ij}$  is assumed to consist of discrete time measurements of a derivative process observed with measurement error  $\varepsilon_{ij}$ , which is modeled via the known function  $g(\cdot)$ . E.g. model (5) is specified with  $g(v, \varepsilon) = \log(v^{\text{kill}} + v^{\text{surv}}) + \varepsilon$ . Finally the subject specific random effects  $\phi_i$  are assumed distributed with a density  $p(\cdot|\eta)$  parametrized by the ‘‘population parameter’’  $\eta$ . Note that measurements  $Y_{ij}$  are conditionally independent given the latent states  $X_{ij} := X_i(t_j)$  and  $\phi_i$ , implying that (6) is a state space model [[Cappé et al., 2006](#)]. It is important to notice that Markovianity of the latent process  $\{X_i(t)\}$  and conditional independence of measurements is essential for the inference methods described in this section. However, these are not required properties for the methodology presented in section 4. The goal of our study is to perform inference for the vector parameter  $\theta = (\eta, \kappa, \sigma_\varepsilon)$ . An important feature of the SDEMEm (6) is its ability to discriminate between the temporal intra-subject variability ( $\kappa$ ), the inter-subjects variability ( $\text{Var}(\phi_i)$ ), and the measurement error variance ( $\sigma_\varepsilon^2$ ). Knowledge of the distinct sources of variation is highly valuable when planning experiments and performing power calculations.

Denote with  $y_i = \{y_{ij}\}_{j=1, \dots, n_i}$  the collection of observations for subject  $i$  and with  $X_i =$

$\{X_{ij}\}_{j=1,\dots,n_i}$  the corresponding values of the latent process. Let  $y = (y_1, \dots, y_M) \in \mathcal{Y}$  denote the full dataset containing measurements for all subjects in the considered group. Standard methods for frequentist as well as Bayesian estimation of the model parameters  $\theta = (\eta, \kappa, \sigma_\varepsilon)$  require the evaluation of the likelihood function  $p(y|\theta) = \prod_{i=1}^M p(y_i|\theta)$ . The hidden Markov structure implies the following derivation

$$\begin{aligned} p(y_i|\theta) &= \int p(y_i|\phi_i; \theta) p(\phi_i|\theta) d\phi_i \\ &= \int \left( \int p(y_i|X_i; \theta) p(X_i|\phi_i; \theta) dX_i \right) p(\phi_i|\theta) d\phi_i \\ &= \int \left( \int \left\{ \prod_{j=1}^{n_i} p(y_{ij}|X_{ij}, \theta) p(X_{i,j}|X_{i,j-1}, \phi_i; \theta) \right\} p(X_{i0}|\phi_i, \theta) dX_i \right) p(\phi_i|\theta) d\phi_i. \end{aligned} \quad (7)$$

Note that the term  $p(X_{i0}|\phi_i, \theta)$  vanishes in either of the cases where  $X_{i0}$  is included among the random effects or is assumed to be a known constant,  $X_{i0} := x_{i0}$ .

In general the likelihood function (7) is not analytically tractable. Thus, inference for SDEMEMs rely on either more specific model assumptions such as the latent processes being Gaussian, or the use of computationally intensive Bayesian methods. [Delattre and Lavielle \[2013\]](#) show how to conduct likelihood inference in SDEMEMs using the stochastic approximate EM algorithm (SAEM) coupled with an extended Kalman filter. [Donnet and Samson \[2014\]](#) propose a particle MCMC algorithm to perform the S-step in SAEM. In either case the use of SAEM requires explicit specification of sufficient summary statistics for the augmented likelihood  $p(y_i, X_i, \phi_i|\theta)$ . While providing fast and accurate inference in models with a latent Gaussian structure, the derivation of the summary statistics is a tedious if not impossible task for more complex models of realistic interest. See [Picchini \[2016\]](#) for a likelihood-free version of SAEM.

Bayesian inference targets the parameter posterior distribution  $\pi(\theta|y) \propto p(y|\theta)\pi(\theta)$  where  $\pi(\theta)$  is the corresponding prior distribution. Bayesian methodology for SDEMEMs was first studied by [Donnet et al. \[2010\]](#) who implemented a Gibbs sampler that applies to the case where the SDE has an explicit solution, and which can be extended to the more general state-space model by using an Euler-Maruyama discretization. A recent review of Bayesian inference methods for SDEMEMs can be found in [Whitaker et al. \[2016\]](#). It is important to notice that MCMC algorithms can be constructed to sample from the exact posterior of  $\theta$ , for models admitting a non-negative unbiased estimator of the likelihood function ([Beaumont, 2003](#), [Andrieu and Roberts, 2009](#)). Here we exemplify a *pseudo-marginal* method [[Andrieu and Roberts, 2009](#)] using sequential Monte Carlo (SMC) to approximate the (intractable) likelihood (7). The key idea is to substitute the intractable  $p(y|\theta)$  with an unbiased non-negative estimate  $\hat{p}(y|\theta)$ , and plug this in an otherwise standard Metropolis-Hastings algorithm (see algorithm 1). Note that

---

**Algorithm 1** A pseudo-marginal MCMC algorithm

---

1. **Input:** a positive integer  $R$ . Fix a starting value  $\theta^*$  or generate it from its prior  $\pi(\theta)$  and set  $\theta_1 := \theta^*$ . Set a kernel  $q(\theta'|\theta)$ . Use algorithm 2 or algorithm 4 to obtain an unbiased estimate  $\hat{p}(y|\theta^*)$  of  $p(y|\theta^*)$ .

**Output:**  $R$  correlated draws from  $\pi(\theta|y)$  (possibly after a burnin).

2. Generate a  $\theta^\# \sim q(\theta^\#|\theta^*)$ . Use algorithm 2 of 4 to obtain an unbiased estimate  $\hat{p}(y|\theta^\#)$  of  $p(y|\theta^\#)$ .

3. Generate a uniform random draw  $u \sim U(0, 1)$ , and calculate the acceptance probability

$$\alpha = \min \left[ 1, \frac{\hat{p}(y|\theta^\#)}{\hat{p}(y|\theta^*)} \times \frac{q(\theta^*|\theta^\#)}{q(\theta^\#|\theta^*)} \times \frac{\pi(\theta^\#)}{\pi(\theta^*)} \right].$$

If  $u > \alpha$ , set  $\theta_{r+1} := \theta_r$  otherwise set  $\theta_{r+1} := \theta^\#$ ,  $\theta^* := \theta^\#$  and  $\hat{p}(y|\theta^*) := \hat{p}(y|\theta^\#)$ . Set  $r := r + 1$  and go to step 4.

4. If  $r \leq R$  repeat steps 2–3 otherwise stop.

---

in sections 5–6 we used a Gaussian kernel  $q(\cdot|\cdot)$  to propose parameters via the adaptive Gaussian random walk algorithm of [Haario et al. \[2001\]](#).

For state-space models, an unbiased estimate of the likelihood function can be obtained using SMC filters, of which two popular examples are the bootstrap filter [[Gordon et al., 1993](#)], adapted in algorithm 2 for hierarchical mixed-effects models, and the auxiliary particle filter ([Pitt and Shephard, 1999](#), [Pitt et al., 2012](#)), of which a version for mixed-effects models is given as algorithm 4 in appendix. Here we describe the bootstrap filter, as it is more approachable for a general audience and it is enough to convey the methodological message. The interested reader is referred to algorithm 4, which is the one we employ to produce our results. The reader might want to consider the notation established in the appendix to implement either a bootstrap filter or an auxiliary particle filter for model (5). Notice that in most cases of practical interest, the forward propagation step in algorithms 2 and 4 requires a numerical scheme, such as Euler-Maruyama (see for example [Golightly and Wilkinson, 2011](#)), though this is not our case as the analytic solutions for  $V_i^{\text{surv}}(t)$  and  $V_i^{\text{kill}}(t)$  for model (5) are known, and therefore their sum  $V_i(t)$  can be simulated exactly. The approximated likelihood is

$$\hat{p}(y|\theta) = \prod_{i=1}^M \hat{p}(y_i|\theta), \quad (8)$$

and when using the bootstrap filter in algorithm 2 we have

$$\hat{p}(y_i|\theta) = \hat{p}(y_{i1}|\theta) \prod_{j=2}^{n_i} \hat{p}(y_{ij}|y_{i,1:j-1}, \theta) = \prod_{j=1}^{n_i} \left( \frac{1}{L} \sum_{l=1}^L w_{ij}^l \right), \quad (9)$$

where  $L$  is the number of particles used to propagate the latent state forward and the  $w_{ij}^l$ 's are importance weights. We have not considered strategies to tune the value of  $L$ , however the reader can refer to [Doucet et al. \[2015\]](#) and [Sherlock et al. \[2015\]](#). Moreover we performed the resampling step using the stratified resampling method of [Kitagawa \[1996\]](#).

---

**Algorithm 2** SMC bootstrap filter for mixed-effects state-space models

---

**Input:** a positive integer  $L$ , a starting value for  $\theta$  and a starting value  $x_0$ . Set time  $t_0 = 0$  and corresponding starting states  $X_{i0} = x_{i0}$ . We use the convention that all steps involving the index  $l$  must be performed for all  $l \in \{1, \dots, L\}$ .

**Output:** all the  $\hat{p}(y_{ij}|y_{i,1:j-1})$ ,  $i = 1, \dots, M$ ;  $j = 1, \dots, n_i$ .

**for**  $i = 1, \dots, M$  **do**

draw  $\phi_i^l \sim p(\phi_i|\theta)$

**if**  $j = 1$  **then**

Sample  $x_{i1}^l \sim p(x_{i1}|x_{i0}, \phi_i^l; \theta)$ .

Compute  $w_{i1}^l = p(y_{i1}|x_{i1}^l)$  and  $\hat{p}(y_{i1}) = \sum_{l=1}^L w_{i1}^l / L$ .

Normalization:  $\tilde{w}_{i1}^l := w_{i1}^l / \sum_{l=1}^L w_{i1}^l$ . Interpret  $\tilde{w}_{i1}^l$  as a probability associated to  $x_{i1}^l$ .

Resampling: sample  $L$  times with replacement from the probability distribution  $\{x_{i1}^l, \tilde{w}_{i1}^l\}$ .

Denote the sampled particles with  $\tilde{x}_{i1}^l$ .

**end if**

**for**  $j = 2, \dots, n_i$  **do**

Forward propagation: sample  $x_{ij}^l \sim p(x_{ij}|\tilde{x}_{i,j-1}^l, \phi_i^l; \theta)$ .

Compute  $w_{ij}^l = p(y_{ij}|x_{ij}^l)$  and normalise  $\tilde{w}_{ij}^l := w_{ij}^l / \sum_{l=1}^L w_{ij}^l$

Compute  $\hat{p}(y_{ij}|y_{i,1:j-1}) = \sum_{l=1}^L w_{ij}^l / L$

Resample  $L$  times with replacement from  $\{x_{ij}^l, \tilde{w}_{ij}^l\}$ . Sampled particles are  $\tilde{x}_{ij}^l$ .

**end for**

**end for**

---

The main distinction between model (6) and other state space models is that latent states are subject specific and can be further decomposed into a time-dependent component  $X_i$  and

a time-independent component  $\phi_i$ . Therefore, when applying SMC we first draw  $\phi_i$  and then, conditionally on such draw, we propagate forward particles corresponding to the states  $X_i$ . As proven by [Del Moral \[2004\]](#) and [Pitt et al. \[2012\]](#) each individual estimate (9) produced by the bootstrap filter and the auxiliary particle filter is unbiased (where the expectation is taken with respect to the distribution used to generate all the random variables employed in the SMC approximation). Since measurements from different subjects are assumed independent, it follows that  $\hat{p}(y|\theta)$  in (8) is an unbiased estimator for  $p(y|\theta)$ . As shown in [Beaumont \[2003\]](#) and [Andrieu and Roberts \[2009\]](#), using an unbiased estimator for  $p(y|\theta)$  is sufficient to ensure that parameter draws produced by algorithm 1 have stationary distribution  $\pi(\theta|y)$  (after a burnin period), for any number of particles  $L$ . This important feature means that algorithms such as 1 are sometimes called “exact-approximate” methods.

## 4 Approximate inference for SDEMEmS using synthetic likelihoods

In this section we discuss approximate Bayesian inference for SDEMEmS using synthetic likelihoods [[Wood, 2010](#)]. Similarly to approximate Bayesian computation (ABC, see [Marin et al., 2012](#) for a review), the synthetic likelihoods methodology is a black-box approach solely relying on simulations from the assumed data-generating model. It is therefore a tool suitable for models having an intractable likelihood. It is important to notice that both ABC and SL do not require the model to have a state-space representation. For instance, both ABC and synthetic likelihoods would apply to a model without assuming Markovian dynamics or conditionally independent measurements, as long as synthetic data from this model can be simulated. Compared to exact likelihood-based methods, the drawbacks of these approximate methodologies is the loss of statistical and computational efficiency and a need to validate the performance of the estimators on a case to case basis.

SL was introduced as a mean to produce inference in models with an intractable likelihood function and/or near-chaotic dynamics. Similarly to ABC, SL relies on a set of carefully selected summary statistics for the data  $s := s(y)$ . However, while in ABC no assumption is made for the distribution of  $s$ , with SL summary statistics are assumed to have a multivariate normal distribution,  $s \sim \mathcal{N}(\mu(\theta), \Sigma(\theta))$  (see [Fasiolo et al. \[2016\]](#) on relaxing such assumption). If this holds true, and if parameters in  $\theta$  can be identified from  $\mu(\theta)$  and  $\Sigma(\theta)$ , then inference for  $\theta$  can be based on the Gaussian likelihood of  $s$  instead of the intractable likelihood of  $y$ . Typically  $\mu(\theta)$  and  $\Sigma(\theta)$  are unknown but can be estimated via simulation. Hence synthetic likelihoods can be viewed as an instance of the simulated method of moments, [McFadden \[1989\]](#).

The implementation of SL is straightforward. For a given  $\theta$ ,  $N$  synthetic datasets  $y^{*1}, \dots, y^{*N}$  are generated independently from the model, hence each entry in the vector  $y^{*n}$  belongs to the space  $\mathcal{Y}$  (see the notation in section 3) and  $\dim(y^{*n}) = \dim(y)$ ,  $n = 1, \dots, N$ . Summary statistics  $s^{*n} = s(y^{*n})$  are computed for each simulated dataset and from these we obtain the moment estimates:

$$\hat{\mu}_N(\theta) = \frac{1}{N} \sum_{n=1}^N s^{*n}, \quad \hat{\Sigma}_N(\theta) = \frac{1}{N-1} \sum_{n=1}^N (s^{*n} - \hat{\mu}_N(\theta))(s^{*n} - \hat{\mu}_N(\theta))'.$$

Note that the only parameter that needs to be specified is  $N$ . When applying SL to SDEMEmS it is important that summary statistics reflect the hierarchical structure of the model. To explain the intra- and inter-individual variance of the model we construct subject-specific summaries  $s_i := s^{\text{intra}}(y_i)$  for  $i = 1, \dots, M$ , as well as summaries that represent inter-individuals variation  $s^{\text{inter}} := s^{\text{inter}}(y_1, \dots, y_M)$ , so that  $s = (s_1, \dots, s_M, s^{\text{inter}})$ .

Approximate normality for summary statistics can often be argued theoretically, e.g. by appealing to the central limit theorem (CLT). If the sample size is small or the summary statistics

do not admit a CLT, then the normal assumption would have to be verified empirically using simulation. We refer to Wood [2010] for further details. Here we follow Price et al. [2017] who proposed a fully Bayesian approach, sampling from the exact posterior  $\pi(\theta|s)$  without incurring any bias caused by the choice of a finite  $N$  (note that “exact” sampling is ensured only if the distribution of  $s$  is really Gaussian). The key feature exploits the idea underlying the pseudo-marginal method discussed in section 3, where an unbiased estimator is used in place of the unknown likelihood function. Price et al. [2017] note that plugging-in the estimates  $\hat{\mu}_N(\theta)$  and  $\hat{\Sigma}_N(\theta)$  into the Gaussian likelihood  $p(s|\theta)$  results in a biased estimator  $p_N(s|\theta)$  of  $p(s|\theta)$ , while one could instead use the unbiased estimator of Ghurye and Olkin [1969] given by

$$\hat{p}(s|\theta) = (2\pi)^{-d/2} \frac{c(d, N-2)}{c(d, N-1)(1-1/N)^{d/2}} |(N-1)\hat{\Sigma}_N(\theta)|^{-(n-d-2)/2} \\ \times \left\{ \psi((N-1)\hat{\Sigma}_N(\theta) - (s - \hat{\mu}_N(\theta))(s - \hat{\mu}_N(\theta))' / (1-1/N)) \right\}^{(N-d-3)/2}. \quad (10)$$

Here  $d = \dim(s)$ ,  $\pi$  denotes the mathematical constant (not the prior),  $N > d + 3$ , and for a square matrix  $A$  the function  $\psi(A)$  is defined as  $\psi(A) = |A|$  if  $A$  is positive definite and  $\psi(A) = 0$  otherwise, where  $|A|$  is the determinant of  $A$ . Finally  $c(k, v) = 2^{-kv/2} \pi^{-k(k-1)/4} / \prod_{i=1}^k \Gamma(\frac{1}{2}(v - i + 1))$ . Algorithm 3 is parallel to algorithm 1, but uses SL to draw from the posterior  $\pi(\theta|s)$  instead of  $\pi(\theta|y)$ .

---

### Algorithm 3 Bayesian synthetic likelihoods

---

**Input:** a positive integer  $R$ . The observed summary statistics  $s$ . Fix a starting value  $\theta^*$  or generate it from the prior  $\pi(\theta)$ . Set  $\theta_1 = \theta^*$ . Choose a kernel  $q(\theta'|\theta)$ .

**Output:**  $R$  correlated samples from  $\pi(\theta|s)$ .

1. Conditionally on  $\theta^*$  generate independently  $N$  summaries  $s^{*1}, \dots, s^{*N}$ , compute moments  $\hat{\mu}_N(\theta^*)$ ,  $\hat{\Sigma}_N(\theta^*)$  and  $\hat{p}(s|\theta^*)$  from (10).
2. Generate a  $\theta^\# \sim q(\theta^\#|\theta^*)$ . Conditionally on  $\theta^\#$  generate independently  $s^{\#1}, \dots, s^{\#N}$ , compute  $\hat{\mu}_N(\theta^\#)$ ,  $\hat{\Sigma}_N(\theta^\#)$  and  $\hat{p}(s|\theta^\#)$ .
3. Generate a uniform random draw  $u \sim U(0, 1)$ , and calculate the acceptance probability

$$\alpha = \min \left[ 1, \frac{\hat{p}(s|\theta^\#)}{\hat{p}(s|\theta^*)} \times \frac{q(\theta^*|\theta^\#)}{q(\theta^\#|\theta^*)} \times \frac{\pi(\theta^\#)}{\pi(\theta^*)} \right].$$

If  $u > \alpha$ , set  $\theta_{r+1} := \theta_r$  otherwise set  $\theta_{r+1} := \theta^\#$ ,  $\theta^* := \theta^\#$  and  $\hat{p}(s|\theta^*) := \hat{p}(s|\theta^\#)$ . Set  $r := r + 1$  and go to step 4.

4. Repeat steps 2–3 as long as  $r \leq R$ .
- 

For the implementation of algorithm 3, note that multiplicative constants such as the  $c(k, v)$ ’s appearing in (10) are independent of  $\theta$  and cancel from the likelihood ratio that defines the acceptance probability. To prevent the MCMC algorithm from reaching a premature halt, we suggest to set  $\hat{p}(s|\theta) := 0$  whenever the argument of  $\psi(\cdot)$  in (10) is not a positive definite matrix (except for the starting value  $\theta^*$ , of course). In the case study, section 5.2, we used algorithm 3 to estimate the model parameters of the SDEMEmS (4) and (5). To the best of our knowledge, this is the first application of the synthetic likelihood methodology to SDEMEmS. The methodology has also been tested with success in the simulation study in section 6. Notice the literature on synthetic likelihoods does not indicate strategies for the identification of informative summary statistics. A procedure for “automatic construction” of summaries could be borrowed from the approximate Bayesian computation literature, see Fearnhead and Prangle [2012].

In section 5 we consider the analysis of real data: a main conclusion is that the size of the data is too small to return accurate inference. This is later confirmed by a simulation study using the same size of data (in section 6). Instead in section 6.1 we show that when considering

a dataset with a larger number of subjects ( $M = 17$ ) it is possible to identify the ground truth parameters using Bayesian synthetic likelihoods.

## 5 Case study

We consider data from a tumor xenography study including four treatment groups (1: chemo therapy, 2: radiation therapy, 3: combination therapy I, 4: combination therapy II), and one untreated control (group 5). Each group consists of 7-8 mice. Mice were followed up on Mondays, Wednesdays, and Fridays for six consecutive weeks or until their tumor volume exceeded 1,000 mm<sup>3</sup>, in which case the mouse was sacrificed as prescribed by the Danish legislation for the use of animals in scientific research. In groups 2 and 4 about half of the mice were sacrificed within the treatment period or shortly after, and due to the reduced sample sizes these are not further considered.

Treatment in equal size doses was applied on days 1, 4, and 6 of the study. Afterwards no treatment was administered. The repeated measurements of tumor volumes in the three remaining groups are shown in Figure 1. It is obvious that growth patterns vary substantially between subjects. In the untreated control group a single mouse with a slowly growing tumor survived for 32 days before sacrifice while all other untreated mice got sacrificed within 10 days. In the active treatment groups we see patterns of decay followed by regrowth which match the characteristic shape of the double exponential curve. In the same groups we also see tumors that appear to grow continuously, unaffected by the treatment. An outlying mouse in group 1 displays a slowly vanishing tumor: for this mouse, most likely the tumor cells never started growing in the first place, so what is measured here is the thickness of the skin, and therefore data for this mouse are not considered in our analyses. Several mice display tumor volumes that are stable over shorter durations of time. These stable periods deviate from the growth patterns of the ordinary simple and double exponential mixed models, but can be explained by the random variations in growth and decay rates which are modeled in the double exponential SDEMEM.

We applied the double exponential SDEMEM (5) to model the post-treatment log-volumes, i.e. starting from (and including) day 6. Separate model fits were obtained for treatment groups 1 and 3. Tumor growth in the untreated controls (group 5) was modeled with the simple exponential SDEMEM (4) starting from day 1 of the study.

For Bayesian analysis of the double exponential SDEMEM (5) we choose a truncated Gaussian prior on the average treatment effect  $\bar{\alpha} \sim \mathcal{N}_{[0,1]}(0.6, 0.2^2)$  which assigns strictly positive probabilities also to values of  $\bar{\alpha}$  equal to zero and one. This is to anticipate that an effective treatment could have the effect that tumors are completely eliminated, while an inefficient treatment might not kill any tumor cells. For all the remaining parameters in (5) we choose as priors  $\log \bar{\beta} \sim \mathcal{N}(0.7, 0.6^2)$ ,  $\log \bar{\delta} \sim \mathcal{N}(0.7, 0.6^2)$ ,  $\sigma_\beta \sim \text{InvGam}(4, 2)$ ,  $\sigma_\delta \sim \text{InvGam}(4, 2)$ ,  $\sigma_\alpha \sim \text{InvGam}(5, 1.5)$ ,  $\gamma \sim \text{InvGam}(5, 7)$ ,  $\tau \sim \text{InvGam}(5, 7)$ , and  $\sigma_\varepsilon \sim \text{InvGam}(2, 1)$ , where  $\text{InvGam}(\cdot)$  denotes the inverse-Gamma distribution. Note that positive model parameters have been reparametrised by their logarithms. See also the Supplementary Material for results obtained with BSL using less informative priors.

### 5.1 Results using exact Bayesian inference

We fitted model (5) separately for groups 1 and 3 using exact Bayesian inference as described in Section 3, where the likelihood function is unbiasedly approximated via the auxiliary particle filter in algorithm 4 (in appendix). For each subject, we set  $v_{i0}$  equal to the corresponding measured volume at day 1; however recall that, by looking at model (5), starting states depend also on  $\alpha_i$ . Algorithm 1 was started at  $\log \bar{\beta} = 1.6$ ,  $\log \bar{\delta} = 1.6$ ,  $\log \bar{\alpha} = -0.36$ ,  $\log \gamma = 0$ ,  $\log \tau = 0$ ,  $\log \sigma_\beta = -0.7$ ,  $\log \sigma_\delta = -0.7$ ,  $\log \sigma_\alpha = -2.3$ ,  $\log \sigma_\varepsilon = 0$ . We used  $L = 2,000$  particles

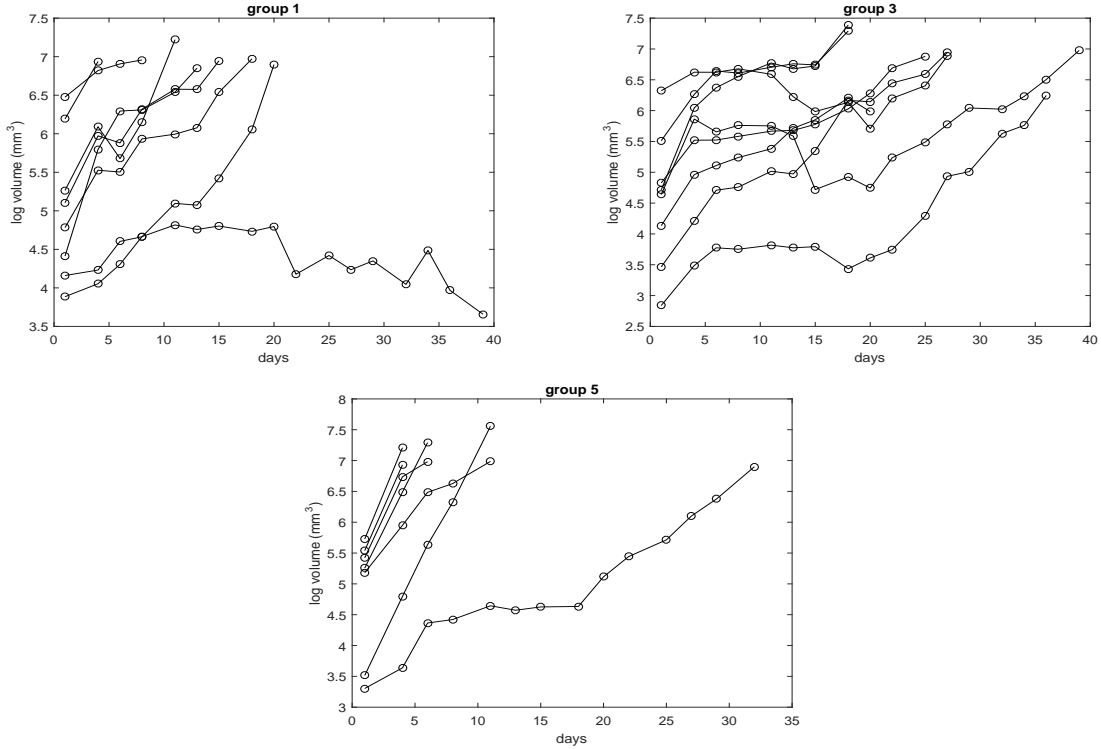


Figure 1: Data of log-volumes ( $mm^3$ ) for three treatment groups.

and  $L_2 = 5$  (the number of particles propagated from each of the  $L$  particles to compute first stage weights, see the description in appendix for details). Chains of length  $R = 20,000$  were produced and the computation took about 53 minutes for treatment group 1 ( $M = 5$ ), and 167 minutes for treatment group 3 ( $M = 8$ ) with a MATLAB code running on a Intel Core i7-4790 3.60 GHz. For both groups average acceptance rates observed during the execution of algorithm 1 were equal to 30%.

Results are shown in Table 1 (we considered the initial 10,000 simulated draws as burnin). Compared to group 1, it is evident that the larger sample size reduces the posterior variability considerably in group 3. The treatment efficacy is estimated at  $\bar{\alpha} = 60\%$  in group 3 and at  $\bar{\alpha} = 52\%$  in group 1, but the difference is not statistically significant, as the posterior for  $\bar{\alpha}$  is very wide in both groups. In section 6.1 we show that having larger sample sizes enables a much better identification of the treatments efficacy  $\bar{\alpha}$ . Note that posteriors for  $\log \bar{\beta}$ ,  $\gamma$ ,  $\tau$  and  $\sigma_\varepsilon$  are informative when compared to their priors. Also, the estimate for  $\bar{\beta}$  is higher in group 1 than in group 3, as it should be by looking at Figure 1, where it is clear that the tumor growth rate in group 1 is faster than in group 3 (recall in group 1 the decaying trajectory was not considered in the analysis). It is reassuring that the measurement error variance is estimated consistently by  $\hat{\sigma}_\varepsilon \simeq 0.1 - 0.2$  in all groups. This means that tumor volumes were measured with a relative accuracy approximately within  $\pm 20\%$ , which is realistic for our experiment. On the other hand, we found the marginal posterior for  $\sigma_\alpha$  to be highly sensitive to the choice of its prior; that is the posterior distribution followed the shape of the prior, regardless of the choice of hyperparameters.

The one-compartment model (4) was fitted to the untreated controls (group 5). The priors were the same as for the corresponding parameters in the two-compartment model (5). Parameter estimates are shown in Table 1. Estimates of the mean population growth rate  $\bar{\beta}$  is again much higher than for groups 1–3, as it should be, see Figure 1. The diffusion coefficient  $\gamma$  is similar to the intensities of the stochasticity for the two-compartment model (as given by  $\gamma$  and  $\tau$ ) and the measurement error variance  $\sigma_\varepsilon$  is compatible with the previously fitted model, which

Table 1: Posterior means and 95% posterior intervals: for each parameter we first report exact Bayesian inference using the particle marginal method PMM and then approximate Bayesian inference using synthetic likelihoods estimation BSL.

	group 1		group 3		group 5	
$\bar{\beta}$	5.81	[3.82,7.83]	3.33	[2.07,4.64]	6.57	[3.72,8.79]
	6.59	[4.90,8.75]	3.93	[2.93,5.04]	8.96	[6.59,11.77]
$\bar{\delta}$	1.84	[0.68,4.59]	1.14	[0.40,2.32]		–
	1.90	[0.53,4.69]	1.52	[0.43,3.68]		
$\bar{\alpha}$	0.52	[0.24,0.84]	0.60	[0.31,0.91]		–
	0.41	[0.13,0.74]	0.47	[0.17,0.84]		
$\gamma$	1.13	[0.66,1.71]	1.09	[0.70,1.52]	1.47	[1.06,2.03]
	1.03	[0.63,1.42]	0.92	[0.56,1.32]	1.25	[0.62,1.83]
$\tau$	1.50	[0.68,2.98]	1.82	[1.02,2.63]		–
	1.51	[0.71,2.77]	1.75	[1.03,2.64]		
$\sigma_\beta$	0.61	[0.23,1.37]	0.51	[0.19,1.67]	0.52	[0.20,1.40]
	0.55	[0.25,1.19]	0.59	[0.23,1.28]	1.10	[0.22,3.02]
$\sigma_\delta$	0.67	[0.24,1.68]	0.76	[0.26,2.23]		–
	0.66	[0.23,1.74]	0.71	[0.25,1.91]		
$\sigma_\alpha$	0.37	[0.16,0.74]	0.29	[0.15,0.48]		–
	0.30	[0.14,0.68]	0.43	[0.14,1.16]		
$\sigma_\varepsilon$	0.22	[0.19,0.30]	0.20	[0.19,0.23]	0.23	[0.20,0.30]
	0.17	[0.10,0.28]	0.11	[0.07,0.17]	0.19	[0.10,0.29]

is reassuring. The variance component  $\sigma_\beta$  was again difficult to identify, which is not surprising given the increased sparsity of the data for this group.

Regardless of the group we fit, notice that the bootstrap filter (which we do not employ here) is known to degenerate when the measurements noise is very small, as in our case with  $\sigma_\varepsilon$  more than an order of magnitude smaller than log-volumes. With a small  $\sigma_\varepsilon$  it is difficult for particles propagated blindly to “hit” the narrow support of the density function for the next observation, hence the use of the auxiliary particle filter.

To make a rough assessment of whether model (5) is realistic compared to the data, we simulated three independent datasets using the posterior means from PMM in Table 1. The simulations are shown in Figures 3 and 4. The overall impression is that model (5) is capable of generating growth dynamics that are similar to the experimental data. Analytical posterior predictive checks (Gelman et al., 2014, chapter 6) are not readily available here, and a motivation is given in the supplementary material, whereas it is possible to produce such checks when using the synthetic likelihood approach, see section 5.2.1. Finally we have verified the chains convergence using the scale reduction factor  $\hat{R}$  [Gelman and Rubin, 1992] as implemented in R’s coda package [Plummer et al., 2006]. We considered three chains initialised at very dispersed values compared to the marginal posteriors. All values for  $\hat{R}$  were below 1.1 except for  $\sigma_\alpha$  ( $\hat{R} = 1.2$ ), hence there seem to be no reason for concern.

## 5.2 Results using synthetic likelihoods

While algorithm 4 produces  $L \times L_2 = 10^4$  trajectories for each iteration of the PMM algorithm, here we use  $N = 3,000$  simulated datasets to construct the synthetic likelihood approximation, and performed Bayesian estimation using  $R = 20,000$  iterations of algorithm 3, as described in section 4. We used the same priors and initial parameter values as in the exact Bayesian analysis. During the execution of the algorithm we observed an acceptance rate of about 30% and the procedure required about 520 seconds for group 3 ( $M = 8$  subjects).

Here we define the components for each individual (vector) statistic  $s_i := s^{\text{intra}}(y_i)$ , see

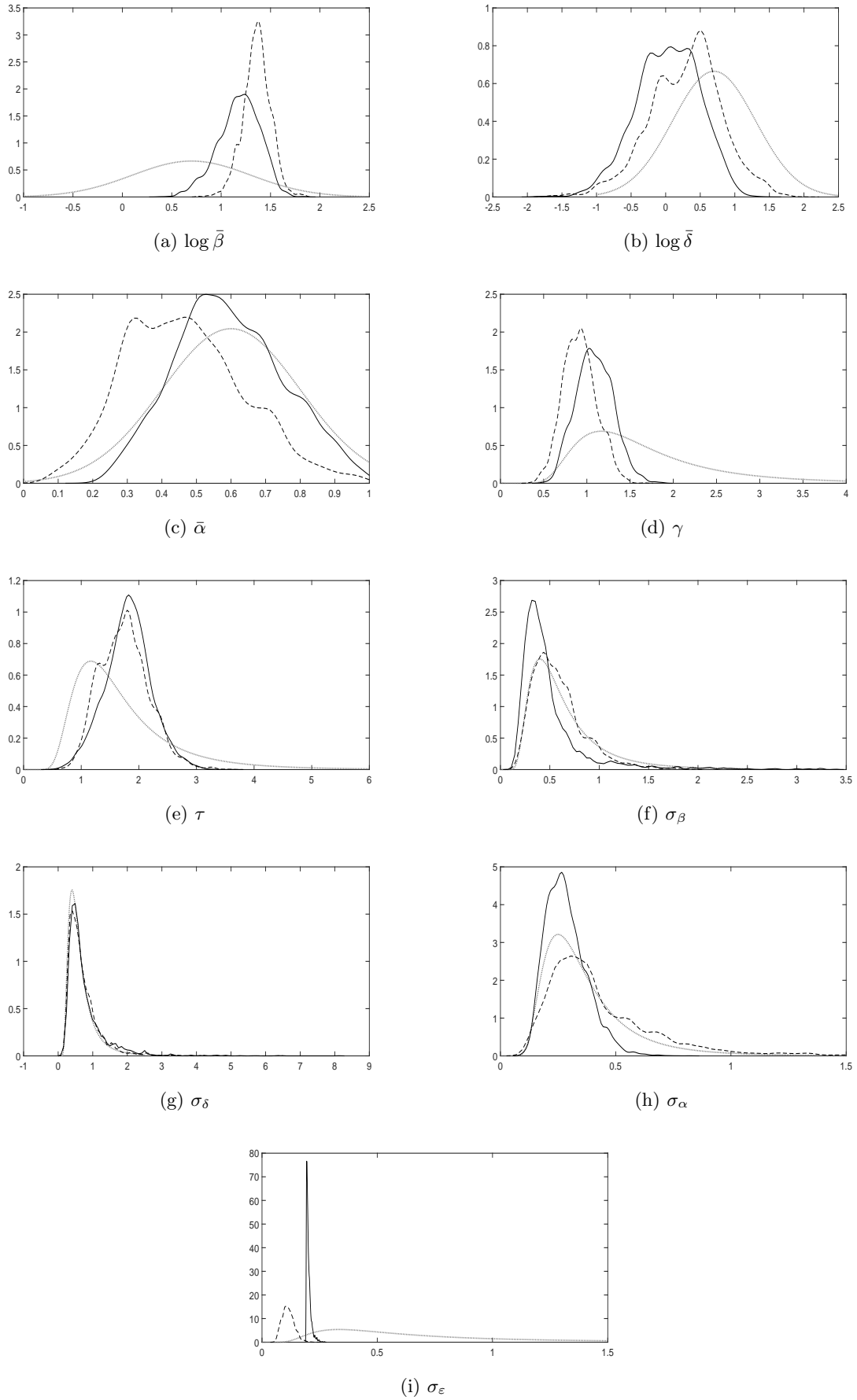


Figure 2: Treatment group 3, exact posteriors via particle marginal method (solid lines), synthetic likelihoods posteriors (dashed) and prior densities (dotted gray). The prior density for  $\sigma_{\epsilon}$  was multiplied by 4 for ease of comparison.

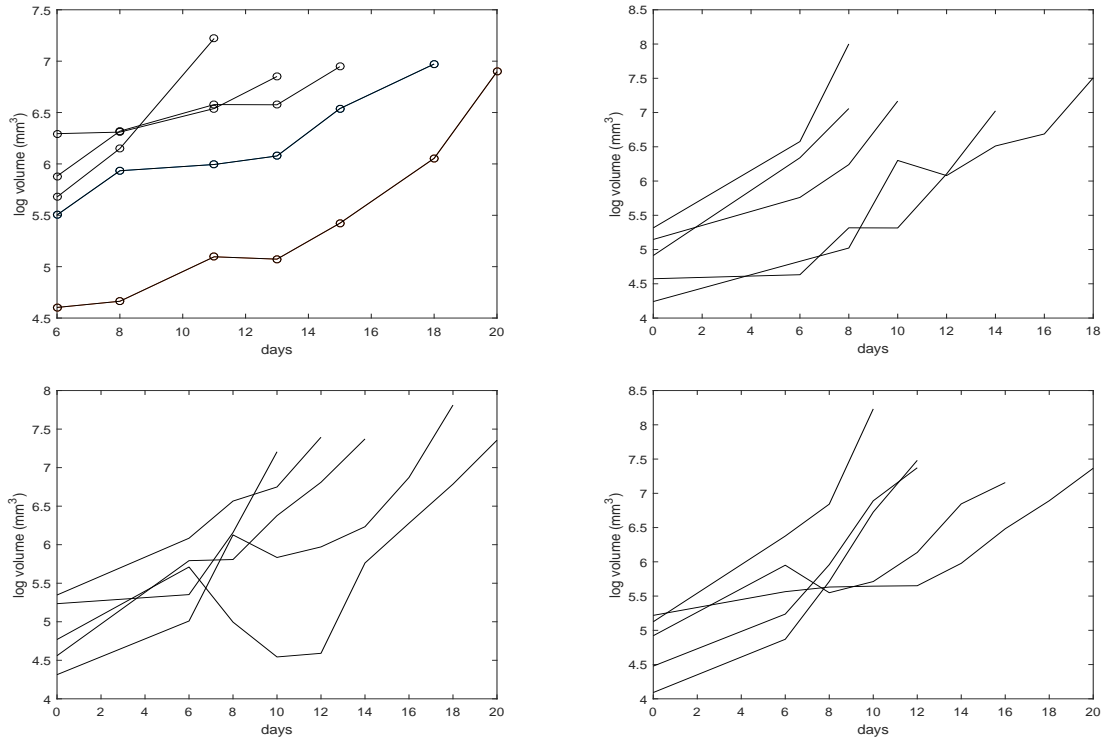


Figure 3: Fitted data in group 1 (top left) and three realizations from model (5) estimated with exact Bayesian methodology (remaining plots). Top left panel does not report data for one excluded mouse. Recall for this group measurements at days 1 and 4 were disregarded during estimation, hence times on abscissas start at day 6.

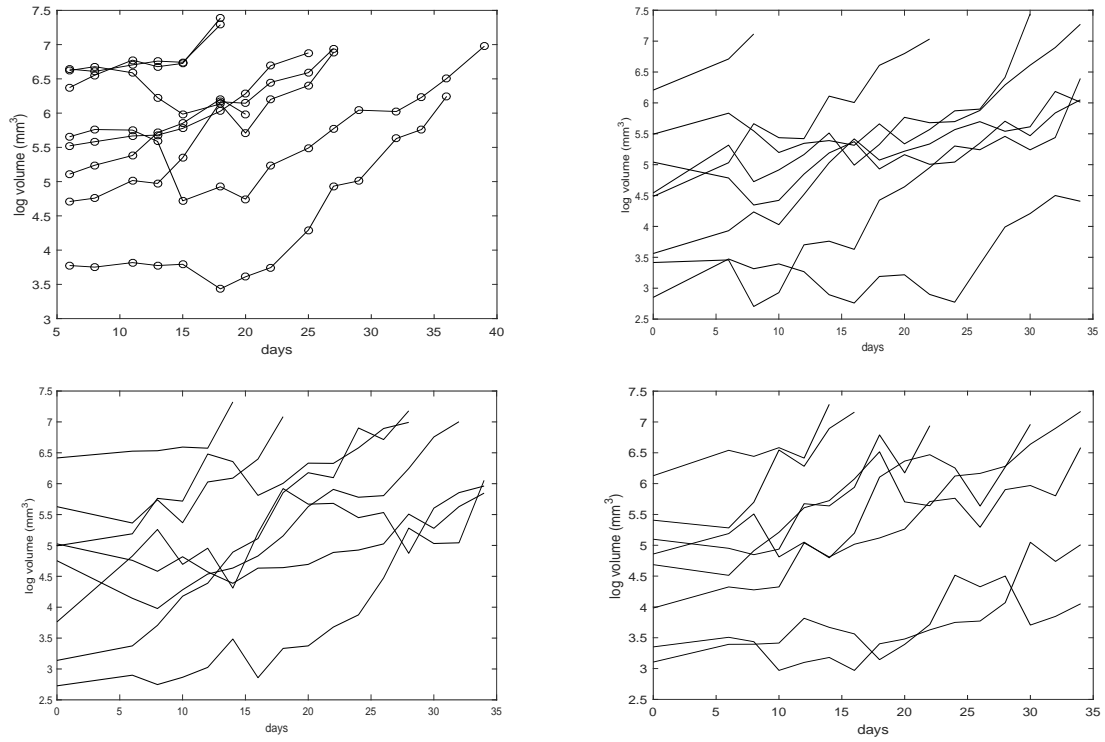


Figure 4: Fitted data in group 3 (top left) and three realizations from model (5) estimated with exact Bayesian methodology (remaining plots). Recall for this group measurements at days 1 and 4 were disregarded during estimation, hence times on abscissas start at day 6.

section 4: (i) the mean absolute deviation for the repeated measurements  $\text{MAD}\{y_{ij}\}_{j=1:n_i}$  (ii) the slope of the line segment connecting the first and the last observation,  $(y_i(t_{n_i}) - y_i(t_1))/(t_{n_i} - t_1)$ ; (iii+iv) the values of the first and second measurements  $y_{i1}$  and  $y_{i2}$ ; (v) the estimated slope of a first order autoregressive fit of the repeated measurements, that is  $\hat{\beta}_{i1}$  from the regression  $E(y_{ij}) = \beta_{i0} + \beta_{i1}y_{i,j-1}$ . Note that when fitting model (4) to the control group, the last summary statistic was dropped to prevent  $\Sigma_N(\theta)$  from being singular (several mice had only two observations so that the second and fifth summary were perfectly correlated). Additional ‘‘population’’ inter-individuals summary statistics  $s^{\text{inter}}$  included are: (i)  $\text{MAD}\{y_{i1}\}_{i=1:M}$ , the mean absolute deviation between subjects at the first time point (day 6 for the active treatment groups and day 1 for the control group); (ii) the same as in (i) but for the second time point; (iii) the same as in (i) but for the last time point. Therefore when fitting group 3 ( $M = 8$  subjects) the total vector of summaries  $s$  contains 43 features, since we have 5 features per subject plus 3 inter-individuals features. In absence of previous literature considering the construction of summary statistics for the considered model, our custom-made summaries follow common sense intuition. For example it seems reasonable to include into  $s^{\text{intra}}(y_i)$  a robust measure of variability (MAD) for individual trajectories; also, since the overall behavior of the trajectories is increasing, we believe the slope of the line connecting first and last observations can give insight on the volume growth rate. Similarly the values of the first two individual measurements could represent an assessment of the initial growth. The first order autoregression is a standard measure of information in dynamic models. Similarly we assess variation between-subjects using  $s^{\text{inter}}$  (useful to quantify the variances of the random effects): to this end we assess the variation between trajectories at several sampling times, in our case by using MAD on measurements from three different times points.

Parameter estimates are presented in Table 1 (considering a burnin of 10,000 iterations) and the approximate marginal posterior distributions for group 3 are in Figure 2. For those posteriors resulting different from the ones obtained with the exact Bayesian methodology, using the corresponding posterior means to produce artificial trajectories does not seem to result in different behaviours. For example Figure 5 (using posterior means estimated with the synthetic likelihoods approach) shows trajectories similar to Figure 4. This suggests that synthetic likelihoods can return reasonable inference for SDEM MEMs, if the summary statistics are well chosen (see also the simulation study in section 6.1). Unfortunately a formal criterion guiding the construction of informative (and Gaussian distributed) summaries is unavailable (though the semi-automatic approach in [Fearnhead and Prangle, 2012](#) could indicate a strategy). Finally, Figure 6 gives normal qq-plots of simulated summaries corresponding to the last draw generated with algorithm 3. All summaries appear fairly close to normality.

We conducted a further investigation (available as Supplementary Material) using less informative priors for  $\log \bar{\delta}$ ,  $\sigma_\beta$  and  $\sigma_\delta$ . The conclusion is that the considered volume of data is not informative enough for these parameters, that is the information carried by the model is unable to depart from the prior information for  $\sigma_\beta$  and  $\sigma_\delta$ . The (log-)elimination rate  $\log \bar{\delta}$  does depart from its prior, but at the expense of increased variability. Finally, we checked the convergence of three chains initialised at the same dispersed values used in the analogous experiment with PMM. For each parameter its  $\hat{R}$  value was below 1.04, hence the chains are converging.

Comparing computational times between BSL and PMM in a fair way is difficult, since the two algorithms have a completely different structure. Both methods perform similarly in terms of acceptance rate (30% in both cases) however in terms of raw numbers, PMM is clearly more intensive since at each MCMC iteration simulation the model is simulated  $L \times L_2 = 10,000$  times, while for BSL the model is simulated only  $N = 3,000$  times (plus the overhead time needed to compute summary statistics out of each simulated trajectory). Given the above, 1,000 MCMC iterations using data from group 3 require 8.35 minutes with PMM and 0.44 minutes with BSL.

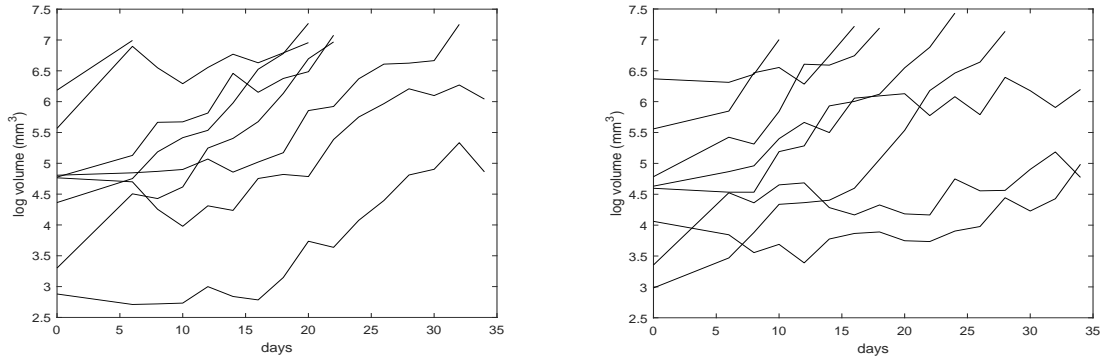


Figure 5: Group 3: two realizations from model (5) estimated with synthetic likelihoods.

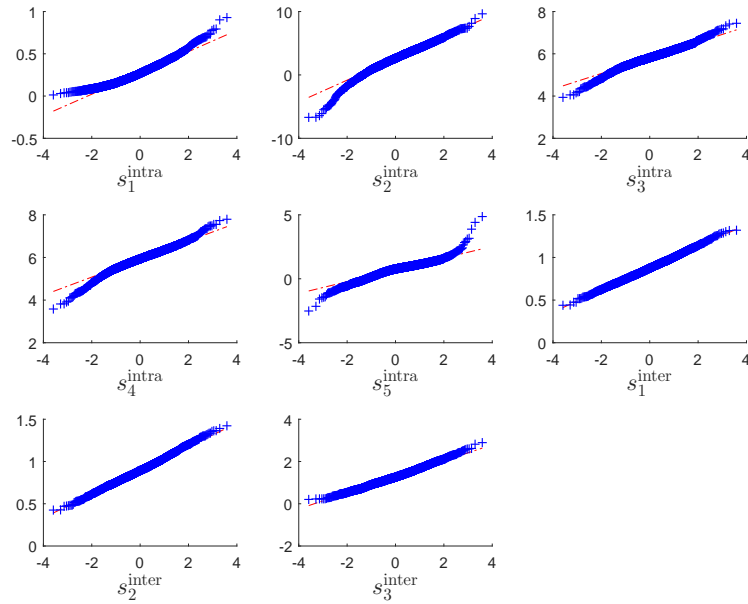


Figure 6: Group 3: normal qq-plots for the intra-individual summary statistics generated for a specific subject from group 3 ( $s_1^{\text{intra}}, \dots, s_5^{\text{intra}}$ ) as well as inter-individual summaries ( $s_1^{\text{inter}}, \dots, s_3^{\text{inter}}$ ). All summaries have been generated in correspondence of the last simulated parameter draw in the MCMC.

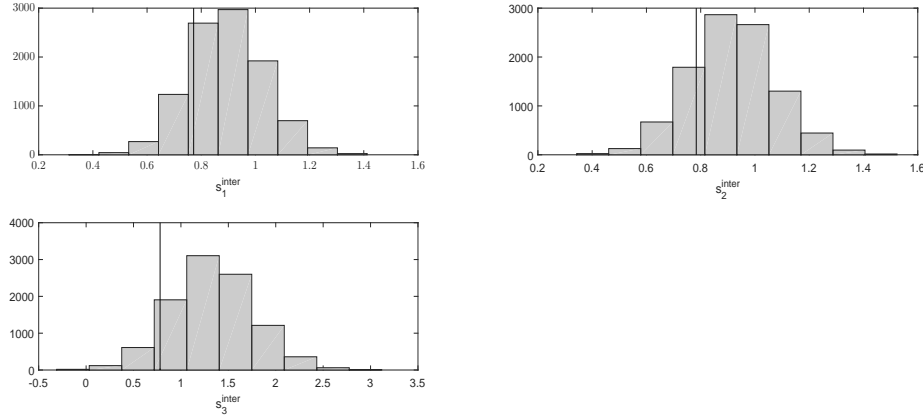


Figure 7: Posterior predictive checks for group 3 using the BSL parameter estimates. Distribution of the simulated statistics for the inter-subjects variability  $s_1^{\text{inter}}$  (top-left),  $s_2^{\text{inter}}$  (top-right) and  $s_3^{\text{inter}}$  (bottom). Vertical lines mark the values for the corresponding statistics from the observed data.

### 5.2.1 Posterior predictive checks

Posterior predictive checks are produced for data in group 3, following the reasoning and notation detailed in the Supplementary Material. We considered the draws produced as output of the BSL algorithm 3 (after burnin) to simulate synthetic summaries from their posterior predictive distribution, and compare the latter to the summaries from observed data. While in posterior predictive checks (Gelman et al., 2014, chapter 6) some features of the model output  $T(y^*)$  should be compared with corresponding features of observed data  $T(y)$ , here the model output is already set to produce model features, that is we take  $T(y^*) \equiv s(y^*)$ . Conditionally on each of the 10,000 draws  $\theta^*$  (after burnin) produced via BSL, we simulate  $s^* \sim N(s^*; \hat{\mu}_N(\theta^*), \hat{\Sigma}_N(\theta^*))$ . Since here we consider group 3, having  $M = 8$  subjects, each  $s^*$  contains 43 features, hence overall we obtain a  $10,000 \times 43$  matrix of features, where each row of the matrix is approximately distributed according to the posterior predictive distribution  $p(s^*|s)$ . Plotting each marginal distribution of  $p(s^*|s)$  is not feasible here, and components pertaining to subject 1 are displayed in Figure 8 together with the corresponding components from the observed  $s$ . Further plots are available as supplementary material. The conclusion here is that for subject 1 all observed summaries are likely to be generated from the estimated model, except for the observed  $s_5^{\text{intra}}$  which seems implausible. However for other subjects (in the supplementary material) the observed summary  $s_5^{\text{intra}}$  is highly probable under  $p(s^*|s)$ .

## 6 Simulation studies

We have run a simulation study where thirty datasets are generated independently from model (5), with ground-truth parameters set to the posterior means obtained with exact Bayesian methodology on group 3, as found in Table 1. The exception being  $\bar{\alpha}$ , set to  $\bar{\alpha} = 0.75$  for consistency with the simulation study conducted in section 6.1. We anticipate that, same as for the previous case study, inference is biased due to the low number of subjects (a necessity here, given the large computational times with PMM when applied to thirty datasets) and that using data having a larger number of subjects produces significant improvements, see section 6.1 having  $M = 17$  subjects.

Each of the thirty datasets has measurements for  $M = 8$  subjects, with observations generated at the same sampling times as for subjects in group 3, and using the same values  $v_{i,0}$  as set for group 3 in the previous sections. For each of the thirty datasets we apply both PMM and BSL, initializing the algorithms at the same starting parameters as in previous analyses. We

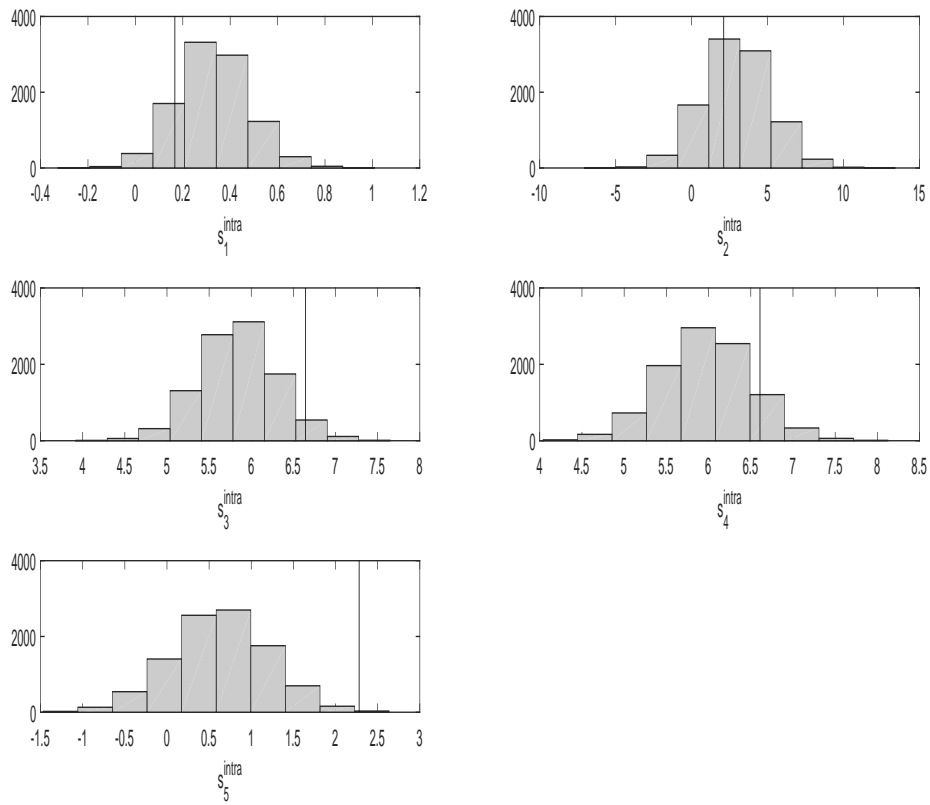


Figure 8: Posterior predictive checks for group 3 using the BSL parameter estimates. Distribution of the simulated statistics for the intra-subjects variability for subject 1:  $s_1^{\text{intra}}$  and  $s_2^{\text{intra}}$  (top),  $s_3^{\text{intra}}$  and  $s_4^{\text{intra}}$  (middle) and  $s_5^{\text{intra}}$  (bottom). Vertical lines mark the values for the corresponding statistics from the observed data.

Table 2: Simulation study: true parameter values ( $\theta_0$ ), median bias and RSME using the particle marginal MCMC method (PMM) and Bayesian synthetic likelihoods (BSL).

	$\bar{\beta}$	$\bar{\delta}$	$\bar{\alpha}$	$\gamma$	$\tau$	$\sigma_\beta$	$\sigma_\delta$	$\sigma_\alpha$	$\sigma_\varepsilon$
$\theta_0$	3.33	1.14	0.75	1.09	1.82	0.51	0.76	0.29	0.20
PMM									
bias	-1.05	-0.54	-0.21	-0.26	-0.51	-0.019	-0.211	0.039	0.121
RMSE	1.09	0.60	0.21	0.27	0.51	0.039	0.213	0.045	0.129
BSL									
bias	-0.93	0.29	-0.28	-0.26	-0.67	-0.039	-0.213	0.001	0.143
RMSE	1.07	0.44	0.30	0.27	0.62	0.053	0.216	0.033	0.161

used the same setup as in the case-study, where PMM uses  $L = 2,000$  particles and  $L_2 = 5$  and the Bayesian synthetic likelihoods approach uses  $N = 3,000$ .

For both methods, we collected the thirty posterior means  $\hat{\theta}_b$ . Also, by denoting with  $\theta_0$  the ground truth parameters, for the  $B = 30$  experiments we compute the median bias, that is the median of the  $B$  differences ( $\hat{\theta}_b - \theta_0$ ) and the root mean square error (RMSE)  $\sqrt{\sum_{b=1}^B (\hat{\theta}_b - \theta_0)^2 / B}$ . Results obtained with PMM and BSL are similar, except for  $\bar{\delta}$ , see Table 2 and Figure 9. It is important to notice that even in a simulation study the “small scale experiment” scenario is statistically challenging. It would be interesting to see results using a larger number of experiments  $B$ ; but unfortunately performing a larger simulation study would be computationally very intensive. Running only thirty simulations required about 41 hours with PMM and 7 hours with BSL. In the next section we explore the effect of increasing the sample size for a single experiment.

## 6.1 Results using larger simulated datasets

Here we run a further simulation study. We consider the problem of treatment identifiability assuming the availability of a larger group of subjects. We simulate two sets of data, each having  $M = 17$  subjects. These two sets are simulated to highlight the role of the parameter  $\bar{\alpha}$ , representing the treatment efficacy at population level, see section 2.1. We produce a first dataset  $\mathcal{D}_1$ , this one emulating a group where the treatment has a low efficacy. For  $\mathcal{D}_1$  we set parameters to the same values as for the PMM estimates for group 1 in Table 1, except for  $\bar{\alpha}$  here set to  $\bar{\alpha} = 0.35$ . The second dataset  $\mathcal{D}_2$  emulates a group where the treatment has high efficacy, by setting  $\bar{\alpha} = 0.75$  and the remaining parameters are equal to the PMM estimates for group 3 in Table 1. For both  $\mathcal{D}_1$  and  $\mathcal{D}_2$  we use Bayesian synthetic likelihoods to estimate parameters, using the same starting parameter values as in previous experiments. Because of the larger number of subjects (hence a larger spread of data points) we use a larger number of simulations  $N$ , here set to  $N = 6,000$ . Figure 10 shows that for both datasets the mean growth rates  $\bar{\beta}$  of the volume of surviving tumor cells are correctly identified, with a higher growth rate for  $\mathcal{D}_1$  than for  $\mathcal{D}_2$  (as it should be for a treatment with lower efficacy), and the two posteriors for  $\bar{\beta}$  are well separated. Compared to the case with  $M = 8$  subjects the treatment mean efficacy  $\bar{\alpha}$  is better identified, as the posteriors are more concentrated (compare against Figure 2). In particular the posterior for  $\bar{\alpha}$  in  $\mathcal{D}_2$  shows a good identification of the ground truth parameter, perhaps thanks to the longer trajectories available in  $\mathcal{D}_2$ , since subjects survive for longer periods. While the true value of  $\bar{\alpha}$  for  $\mathcal{D}_1$  is not improbable but also not very likely, we can definitely notice a major shift in the results from the case of  $M = 8$  subjects (as seen in Figure 2): here the separation between the two marginal posteriors suggests that we could obtain more accurate inferences for treatments efficacy in real data, should larger experiments be conducted. We also notice that the residual variability  $\sigma_\varepsilon$  is difficult to identify with high precision. When comparing the inference for  $\sigma_\varepsilon$

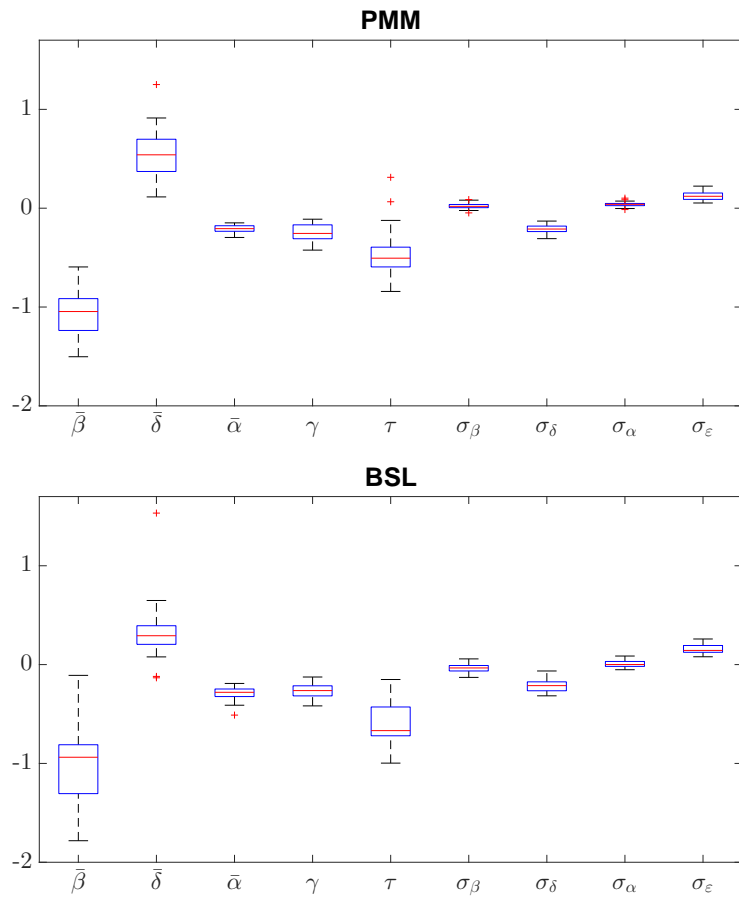


Figure 9: Simulation study with  $M = 8$  subjects: top, boxplots of the parameter estimates bias obtained with PMM; bottom, boxplots of the bias when using Bayesian synthetic likelihoods.

with the real data results in Figure 2, we conjecture that for the real data experiment (where  $M$  is small) the inference injects considerable uncertainty into the estimate of  $\bar{\alpha}$ . We therefore deduce that for small  $M$  we underestimate the residual variability, as a non-negligible fraction of the total variability is assigned to the treatment variability. For the simulated data with  $M = 17$  we have the opposite situation, where  $\bar{\alpha}$  is estimated more precisely, this producing an enlarged residual variability  $\sigma_\varepsilon$ . However the true value for the latter is not well captured, therefore it seems that we cannot obtain precise estimates simultaneously for both parameters.

## 7 Summary

We have introduced a new mixed effects model for the analysis of repeated measurements of tumor volumes in mice in a tumor xenograft study. For each subject the dynamics for the exact, unobservable, tumor volumes are modeled by stochastic differential equations (SDEs), while observed volumes are assumed perturbed with measurement error. The resulting model is a stochastic differential mixed effects model (SDEMEM), which is of state-space type. SDEMEMs provide a very useful representation for repeated measurement data since they are able to distinguish several sources of variability, in the present example: intra-individual temporal variability, biologic variability between subjects, and measurement error (residual variability). We considered two different SDEMEMs: one for unperturbed growth, modelling an untreated control group, and one for tumor (re)growth following an active treatment such as chemo- or radiation therapy. The former is a one-compartment model while the latter is a two compartments model. The two compartments represent the unobserved fraction of tumor cells that has been killed by the treatment ( $V^{\text{kill}}$ ) and the unobserved fraction that has survived the treatment ( $V^{\text{surv}}$ ), respectively. Hence the model extends the classical double exponential model by including random perturbations in the growth dynamics.

Parameter inference for the SDEMEM is difficult for several reasons. One is the intractability of the likelihood function. Another reason is that model parameters are difficult to identify, since data consist of noisy measurements of the total tumor  $V = V^{\text{surv}} + V^{\text{kill}}$ , not the separate compartments. Finally, most tumor xenograft studies are performed with small sample sizes. We have considered methods for exact and approximate Bayesian inference to overcome this. In particular, we have compared approximate Bayesian inference using the synthetic likelihoods (SL) approach (Wood, 2010, Price et al., 2017) to exact Bayesian inference using a particle marginal method (Andrieu and Roberts, 2009). SL bases the inference on the likelihood function of normally distributed summary statistics, instead of the intractable likelihood function of the actual data. The efficiency of the resulting estimator relies on the choice of the summary statistics. For the application to SDEMEMs we advocated the use of subject specific summaries, which can be further comprised over groups by taking averages and computing covariances. In an application to a tumor xenograft study with two active treatment groups and an untreated control, comprising data from 5-8 subjects, we found that Bayesian synthetic likelihoods performed similarly to exact Bayesian inference, indicating that our choice of summary statistics was appropriate. A further advantage of synthetic likelihoods is that, unlike exact particle-based inference, it can be applied to models other than the state-space type, thus inference could be extended to other stochastic growth rate models than state-space SDEMEMs.

A finding from the case study was that larger sample sizes are needed to identify all model parameters and obtain accurate estimates of the treatment contrasts. This was confirmed in simulation studies with data from eight and seventeen subjects in each group, respectively. Although we recommend larger sample sizes for obtaining valid statistical inference, Bayesian inference may still be used to perform exploratory analyses in small scale experiments. In the latter case, judicious informative priors based on subject matter expertise may compensate for the otherwise too small sample size.

In conclusion SDEMEMs allow for mechanistic modeling of tumor growth and response to

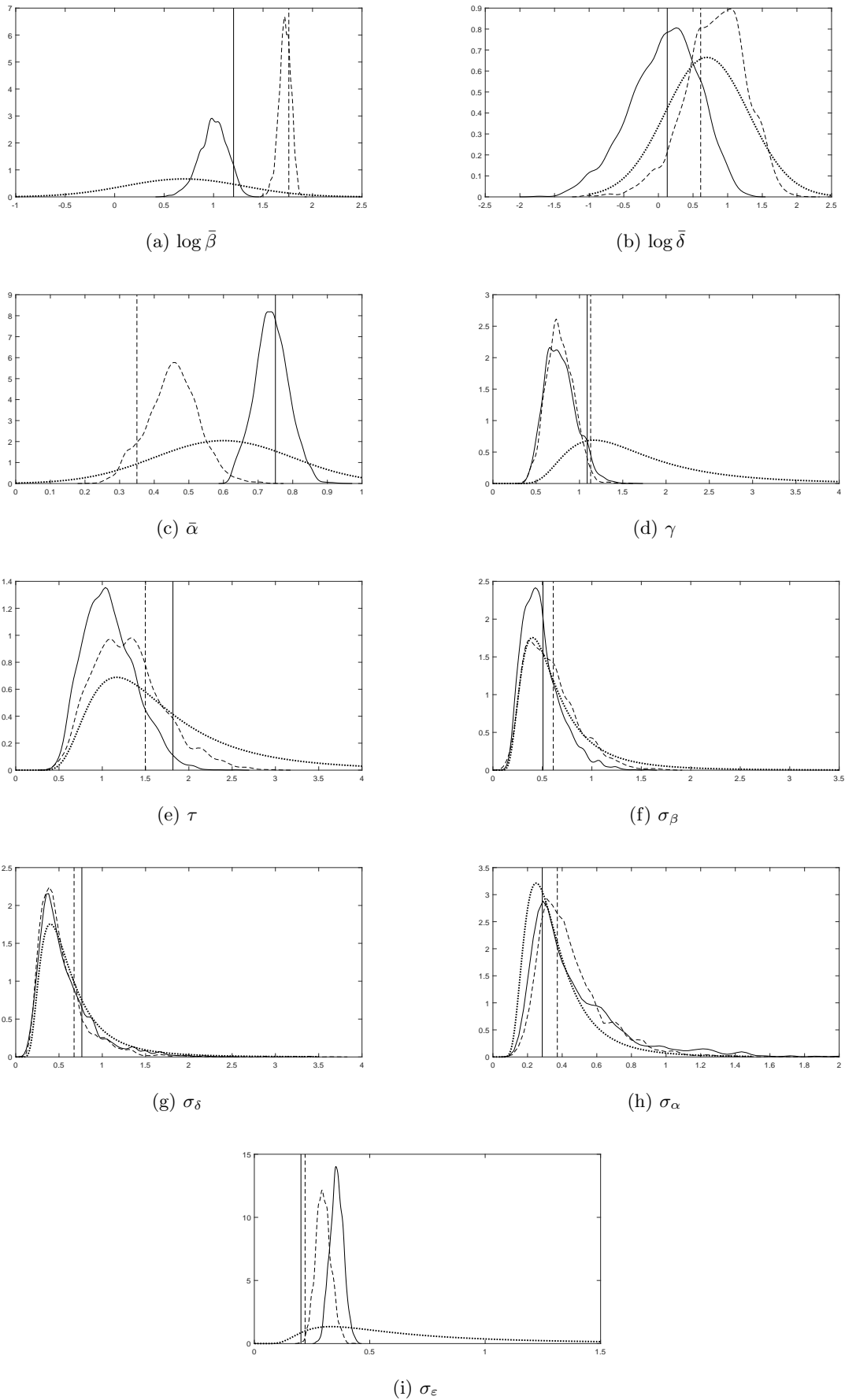


Figure 10: Posteriors based on simulated data  $\mathcal{D}_1$  (dashed curves) and based on simulated data  $\mathcal{D}_2$  (solid lines) obtained with Bayesian synthetic likelihoods. Dashed vertical lines indicate ground-truth parameters used for  $\mathcal{D}_1$ , while solid vertical lines are ground-truth parameters used for  $\mathcal{D}_2$ . Dotted lines denote prior densities.

treatment including natural sources of variability. These may be useful for power calculations and optimal design, even in studies where more robust statistical methods are preferred for confirmatory data analysis.

## Acknowledgements

Research was partially supported by the Swedish Research Council (VR grant 2013-05167). We would like to thank the research team at the Center for Nanomedicine and Theranostics, DTU Nanotech, Denmark for providing the data for the case study and for introducing us to the problem of making inference from tumor xenography experiments.

## A Auxiliary particle filter for mixed-effects state-space models

In algorithm 4 we give a version of the auxiliary particle filter (APF), adapted for mixed-effects state-space models (SSM). APF was initially proposed by Pitt and Shephard [1999] to make inference for the latent state of a SSM. For the purpose of obtaining an unbiased approximation of the likelihood function, we consider Pitt et al. [2012]. For the case where the SSM has dynamics driven by a stochastic differential equation with no closed form solution, an appealing proposal function is given in Golightly and Wilkinson [2011]. Same as for algorithm 2, we assume a fixed initial state  $x_0$ , but otherwise sampling of particles  $x_0^l \sim p(x_0)$  should be performed.

For *each* of the  $L$  particles available at time  $t_{i,j-1}$ , the function `FirstStagePropagate` propagates forward  $L_2$  particles to the next time  $t_{i,j}$ , then computes the sample mean from the cloud of  $L_2$  particles. Based on the results of this preliminary propagation, a second propagation  $x_{ij}^l \sim p(x_{ij}|x_{i,j-1}^k)$  simulates particles forward starting from those particles that appear to be promising candidates, according to the preliminary “exploration” conducted via the first stage propagation (i.e. the promising particles are those having indices  $k^l$  sampled according the first stage weights  $\omega$ ). The obtained approximate likelihood  $\hat{p}(y|\theta) = \prod_{i=1}^M \{\hat{p}(y_{i1}|\theta) \prod_{j=2}^{n_1} \hat{p}(y_{ij}|y_{i,1:j-1}, \theta)\}$  is unbiased (Pitt, 2002, Pitt et al., 2012).

With reference to model (5) the notation in algorithm 4 is as follows: the starting total volume is  $V_{i0} := V_i^{\text{surv}}(0) + V_i^{\text{kill}}(0)$  where  $V_i^{\text{surv}}(0) = (1 - \alpha_i)v_{i0}$  and  $V_i^{\text{kill}}(0) = \alpha_i v_{i0}$ . Then we have  $x_{ij} := \log V_{ij}$ , hence  $\bar{x}_{ij}^l := \sum_{l_2=1}^{L_2} (\log V_{ij}^{l_2})/L_2$ , so that  $p(y_{ij}|x_{ij}^l) \equiv \mathcal{N}(y_{ij}; x_{ij}^l, \sigma_\varepsilon^2)$  and  $p(y_{ij}|\bar{x}_{ij}^l) \equiv \mathcal{N}(y_{ij}; \bar{x}_{ij}^l, \sigma_\varepsilon^2)$ . In general, for any particle and regardless of whether this is  $x_{ij}^l := \log V_{ij}^l$  or  $x_{ij}^{l_2} := \log V_{ij}^{l_2}$ , we have that  $V_{ij}^l := (V_{ij}^{\text{kill}})^l + (V_{ij}^{\text{surv}})^l$  (respectively  $V_{ij}^{l_2} := (V_{ij}^{\text{kill}})^{l_2} + (V_{ij}^{\text{surv}})^{l_2}$ ), that is the indices  $l$  (resp.  $l_2$ ) obtained when resampling the total volumes are used to select the “surviving” and “killed” states. Finally note that for algorithm 4 (and similarly for algorithm 2) the “best” particles for the total volumes are not necessarily the best particles for  $V^{\text{surv}}$  and  $V^{\text{kill}}$ , when these are considered separately.

---

**Algorithm 4** Auxiliary particle filter for mixed-effects state-space models
 

---

**Input:** positive integers  $L$  and  $L_2$ , a value for  $\theta$ . Set time  $t_0 = 0$ . Everything that follows is conditional on the current value of  $\theta$ , which is therefore removed from the notation.

**Output:** all the  $\hat{p}(y_{ij}|y_{i,1:j-1})$ ,  $i = 1, \dots, M$ ;  $j = 1, \dots, n_i$ .

**for**  $i = 1, \dots, M$  **do**

draw  $\phi_i^l \sim p(\phi_i)$  for all  $l \in \{1, \dots, L\}$ . Form  $x_{i0}^l := x_{i0}(\phi_i^l)$  accordingly and  $x_{i0} := (x_{i0}^1, \dots, x_{i0}^L)$ . Set normalised weights  $\tilde{w}_{i0}^l = 1/L$  for all  $l \in \{1, \dots, L\}$ .

**if**  $j = 1$  **then**

$\bar{x}_{i1} := \text{FirstStagePropagate}(x_{i0}, L, L_2)$

Compute first stage weights  $\omega_{i1}^l = p(y_{i1}|\bar{x}_{i1}^l)\tilde{w}_{i0}^l$ .

Normalization:  $\tilde{\omega}_{i1}^l := \omega_{i1}^l / \sum_{l=1}^L \omega_{i1}^l$ . Interpret  $\tilde{\omega}_{i1}^l$  as the probability for index  $l_{i1}$  associated to  $\bar{x}_{i1}^l$ .

Resampling: sample  $L$  times with replacement from the probability distribution  $\{l_{i1}, \tilde{\omega}_{i1}^l\}$ . Denote the sampled indeces with  $k^1, \dots, k^L$ .

Second propagation: sample  $x_{i1}^l \sim p(x_{i1}|x_{i0}^{k^l})$ .

Compute second stage weights  $w_{i1}^l = p(y_{i1}|x_{i1}^l)/p(y_{i1}|\bar{x}_{i1}^l)$ .

Compute  $\hat{p}(y_{i1}) = \left( \frac{\sum_{l=1}^L w_{i1}^l}{L} \right) \sum_{l=1}^L \omega_{i1}^l$ .

Normalise:  $\tilde{w}_{i1}^l := w_{i1}^l / \sum_{l=1}^L w_{i1}^l$ .

**end if**

**for**  $j = 2, \dots, n_i$  **do**

$\bar{x}_{ij} := \text{FirstStagePropagate}(x_{i,j-1}, L, L_2)$

Compute  $\omega_{ij}^l = p(y_{ij}|\bar{x}_{ij}^l)\tilde{w}_{i,j-1}^l$ .

Normalization:  $\tilde{\omega}_{ij}^l := \omega_{ij}^l / \sum_{l=1}^L \omega_{ij}^l$ . Interpret  $\tilde{\omega}_{ij}^l$  as the probability for index  $l_{ij}$  associated to  $\bar{x}_{ij}^l$ .

Resampling: sample  $L$  times with replacement from the probability distribution  $\{l_{ij}, \tilde{\omega}_{ij}^l\}$ . Denote the sampled indeces with  $k^1, \dots, k^L$ .

Second propagation: sample  $x_{ij}^l \sim p(x_{ij}|x_{i,j-1}^{k^l})$ .

Compute second stage weights  $w_{ij}^l = p(y_{ij}|x_{ij}^l)/p(y_{ij}|\bar{x}_{ij}^l)$ .

Compute  $\hat{p}(y_{ij}|y_{i,1:j-1}) = \left( \frac{\sum_{l=1}^L w_{ij}^l}{L} \right) \sum_{l=1}^L \omega_{ij}^l$ .

Normalise:  $\tilde{w}_{ij}^l := w_{ij}^l / \sum_{l=1}^L w_{ij}^l$ .

**end for**

**end for**

---

**Function**  $\bar{x}_{ij} := \text{FirstStagePropagate}(x_{i,j-1}, L, L_2)$ :

**for**  $l = 1, \dots, L$  **do**

Sample  $x_{ij}^{l_2} \sim p(x_{ij}|x_{i,j-1}^l)$ , for each  $l_2 \in \{1, \dots, L_2\}$ .

Compute  $\bar{x}_{ij}^l := \sum_{l_2=1}^{L_2} x_{ij}^{l_2} / L_2$ .

**end for**

Return  $\bar{x}_{ij} := (\bar{x}_{ij}^1, \dots, \bar{x}_{ij}^L)$ .

---

## References

- C. Andrieu and G. Roberts. The pseudo-marginal approach for efficient Monte Carlo computations. *The Annals of Statistics*, pages 697–725, 2009.
- M. Beaumont. Estimation of population growth or decline in genetically monitored populations. *Genetics*, 164(3):1139–1160, 2003.
- O. Cappé, E. Moulines, and T. Rydén. *Inference in hidden Markov models*. Springer Science & Business Media, 2006.
- P. Del Moral. *Feynman-Kac formulae: genealogical and interacting particle systems with applications*. New York: Springer, 2004.
- M. Delattre and M. Lavielle. Coupling the SAEM algorithm and the extended Kalman filter for maximum likelihood estimation in mixed-effects diffusion models. *Statistics and its interface*, 6(4):519–532, 2013.
- E. Demidenko. The assessment of tumour response to treatment. *Journal of the Royal Statistical Society: Series C (Applied Statistics)*, 55(3):365–377, 2006.
- E. Demidenko. Three endpoints of in vivo tumour radiobiology and their statistical estimation. *International journal of radiation biology*, 86(2):164–173, 2010.
- E. Demidenko. *Mixed models: theory and applications with R*. John Wiley & Sons, 2013.
- S. Donnet and A. Samson. A review on estimation of stochastic differential equations for pharmacokinetic/pharmacodynamic models. *Advanced Drug Delivery Reviews*, 65(7):929–939, 2013.
- S. Donnet and A. Samson. Using PMCMC in EM algorithm for stochastic mixed models: theoretical and practical issues. *Journal de la Société Française de Statistique*, 155(1):49–72, 2014.
- S. Donnet, J. Foulley, and A. Samson. Bayesian analysis of growth curves using mixed models defined by stochastic differential equations. *Biometrics*, 66(3):733–741, 2010.
- A. Doucet, M. Pitt, G. Deligiannidis, and R. Kohn. Efficient implementation of Markov chain Monte Carlo when using an unbiased likelihood estimator. *Biometrika*, 2015. doi: doi:10.1093/biomet/asu075.
- M Fasiolo, S Wood, F Hartig, and M Bravington. An extended empirical saddlepoint approximation for intractable likelihoods. *arXiv:1601.01849*, 2016.
- P. Fearnhead and D. Prangle. Constructing summary statistics for approximate Bayesian computation: semi-automatic approximate Bayesian computation (with discussion). *Journal of the Royal Statistical Society series B*, 74:419–474, 2012.
- C. Fuchs. *Inference for Diffusion Processes: With Applications in Life Sciences*. Springer Science & Business Media, 2013.
- A Gelman and D Rubin. Inference from iterative simulation using multiple sequences. *Statistical Science*, pages 457–472, 1992.
- A Gelman, J Carlin, H Stern, D Dunson, A Vehtari, and D Rubin. *Bayesian data analysis*. CRC Press, third edition, 2014.
- S. Ghurye and I. Olkin. Unbiased estimation of some multivariate probability densities and related functions. *The Annals of Mathematical Statistics*, pages 1261–1271, 1969.

- A. Golightly and D. Wilkinson. Bayesian parameter inference for stochastic biochemical network models using particle Markov chain Monte Carlo. *Interface Focus*, 1(6):807–820, 2011.
- N. Gordon, D. Salmond, and A. Smith. Novel approach to nonlinear/non-Gaussian Bayesian state estimation. In *Radar and Signal Processing, IEE Proceedings F*, volume 140, pages 107–113, 1993.
- H. Haario, E. Saksman, and J. Tamminen. An adaptive Metropolis algorithm. *Bernoulli*, pages 223–242, 2001.
- D. Heitjan. Generalized Norton-Simon models of tumour growth. *Statistics in medicine*, 10(7):1075–1088, 1991.
- D. Heitjan, A. Manni, and R. Santen. Statistical analysis of in vivo tumor growth experiments. *Cancer Research*, 53(24):6042–6050, 1993.
- G. Kitagawa. Monte Carlo filter and smoother for non-Gaussian nonlinear state space models. *Journal of computational and graphical statistics*, 5(1):1–25, 1996.
- M. Kong and J. Yan. Modeling and testing treated tumor growth using cubic smoothing splines. *Biometrical Journal*, 53(4):595–613, 2011.
- T. Laajala, J. Corander, N. Saarinen, K. Mäkelä, S. Savolainen, M. Suominen, E. Alhoniemi, S. Mäkelä, M. Poutanen, and T. Aittokallio. Improved statistical modeling of tumor growth and treatment effect in preclinical animal studies with highly heterogeneous responses in vivo. *Clinical Cancer Research*, 18(16):4385–4396, 2012.
- J. Marin, P. Pudlo, C. Robert, and R. Ryder. Approximate Bayesian computational methods. *Statistics and Computing*, 22(6):1167–1180, 2012.
- D. McFadden. A method of simulated moments for estimation of discrete response models without numerical integration. *Econometrica*, 57(5):995–1026, 1989.
- J Péron, M Buyse, B Ozenne, L Roche, and P Roy. An extension of generalized pairwise comparisons for prioritized outcomes in the presence of censoring. *Statistical methods in medical research*, 2016. doi: 10.1177/0962280216658320.
- U. Picchini. Likelihood-free stochastic approximation EM for inference in complex models. 2016. arXiv:1609.03508.
- M. Pitt. Smooth particle filters for likelihood evaluation and maximisation. Technical Report 651, 2002.
- M. Pitt and N. Shephard. Filtering via simulation: Auxiliary particle filters. *Journal of the American statistical association*, 94(446):590–599, 1999.
- M. Pitt, R. dos Santos Silva, P. Giordani, and R. Kohn. On some properties of Markov chain Monte Carlo simulation methods based on the particle filter. *Journal of Econometrics*, 171(2):134–151, 2012.
- M Plummer, N Best, K Cowles, and K Vines. CODA: Convergence diagnosis and output analysis for MCMC. *R News*, 6(1):7–11, 2006.
- L. Price, C. Drovandi, A. Lee, and D. Nott. Bayesian synthetic likelihood. *Journal of Computational and Graphical Statistics*, 2017. doi: 10.1080/10618600.2017.1302882.
- C. Sherlock, A. Thiery, G. Roberts, and J. Rosenthal. On the efficiency of pseudo-marginal random walk Metropolis algorithms. *The Annals of Statistics*, 43(1):238–275, 2015.

- M. Stuschke, V. Budach, M. Bamberg, and W. Budach. Methods for analysis of censored tumor growth delay data. *Radiation research*, 122(2):172–180, 1990.
- G. Whitaker, A. Golightly, R. Boys, and C. Sherlock. Bayesian inference for diffusion driven mixed-effects models. *Bayesian Analysis*, 2016.
- S. Wood. Statistical inference for noisy nonlinear ecological dynamic systems. *Nature*, 466(7310):1102–1104, 2010.
- J. Wu. Confidence intervals for the difference of median failure times applied to censored tumor growth delay data. *Statistics in Biopharmaceutical Research*, 3(3):488–496, 2011.
- J. Wu and P. Houghton. Assessing cytotoxic treatment effects in preclinical tumor xenograft models. *Journal of biopharmaceutical statistics*, 19(5):755–762, 2009.
- C. Xia, J. Wu, and H. Liang. Model tumor pattern and compare treatment effects using semi-parametric linear mixed-effects models. *Journal of Biometrics & Biostatistics*, 2013, 2013.
- L. Zhao, M. Morgan, L. Parsels, J. Maybaum, T. Lawrence, and D. Normolle. Bayesian hierarchical changepoint methods in modeling the tumor growth profiles in xenograft experiments. *Clinical Cancer Research*, 17(5):1057–1064, 2011.

## Supplementary Material

### Posterior predictive checks

We discuss posterior predictive checks for both the pseudo-marginal Metropolis algorithm (PMM) and for Bayesian synthetic likelihoods (BSL). Performing posterior predictive checks when the likelihood is approximated using particle filters, as in the PMM algorithm, is not trivial. Denote with  $y^*$  a simulated realization from the hypothesized data-generating model, that is  $y^* \sim p(y^*|\theta)$  where  $p(y|\theta)$  denotes the likelihood function and  $y$  the observed data. The posterior predictive distribution  $p(y^*|y)$ , as defined by Gelman et al., 2014 chapter 6, is given by

$$p(y^*|y) = \int p(y^*|\theta)\pi(\theta|y)d\theta$$

where  $\pi(\theta|y)$  is the posterior of  $\theta$ . We would like to first simulate  $\theta^* \sim \pi(\theta|y)$  (which may be obtained from the PMM output, after burnin), and next  $y^* \sim p(y^*|\theta^*)$ . This way we obtain a realization from  $p(y^*|y)$ . To compare the predicted distribution of  $y^*$  with the observed data  $y$ , we choose summary statistics, say to compare  $T(y)$  to the distribution of  $T(y^*)$  (not to be confused with the summaries used in the synthetic likelihood approach,  $s(y)$ ).

Clearly, since  $p(y|\theta)$  is unknown in closed form, it must be approximated, for example using algorithms 2-4 to return  $\hat{p}(y|\theta)$ . In our case, because of the dependence of data  $y$  on unobservables  $(X, \phi)$ , and because of the multidimensional integral in (7) each likelihood term has an unknown distribution and we cannot sample a  $y^*$  from  $\hat{p}(y|\theta)$ . A possibility, which we leave for the interested reader, is to sample for the generic subject  $i$  an  $X_i^*$  from the filtering distribution  $p(X_i|y_i; \theta^*)$ , where  $\theta^*$  is a draw obtained via PMM, then form  $y_{ij}^* = g(X_{ij}^*, \varepsilon_{ij}^*)$ , with  $\varepsilon_{ij} \sim N(0, \sigma_{ij}^2)$  following the notation in model (6). Here  $X_i^*$  is a trajectory that it is possible to obtain as a by-product of either algorithm 2 or 4, by sampling a single index  $l'$  from the cloud of particles obtained at the last time point  $t_{in_i}$  then follow the genealogy of  $l'$  backwards up to time  $t_0 = 0$ . The sequence of ancestors of the particle  $l'$  provides a single path from  $p(X_i|y_i; \theta^*)$ .

For BSL the approach is much simpler as we can consider  $T(y) \equiv s(y)$ . In this case we have

$$p(s^*|s) = \int p(s^*|\theta)\pi(\theta|s)d\theta$$

where  $s := s(y)$ . It is possible to simulate from an approximation to  $p(s^*|s)$ , as we explain below. First note that the parameters  $\theta^*$  sampled via the BSL algorithm 3 are constructed using the (unbiased) likelihood (10) which is clearly not Gaussian. Therefore, in order to sample from (an approximation to the) posterior predictive distribution, we need to consider the "biased" Gaussian likelihood  $p_N(s|\theta^*) := \mathcal{N}(\theta^*; \hat{\mu}_N(\theta^*), \hat{\Sigma}_N(\theta^*))$ , with moments given in section 4. Given the previous remark, for any  $\theta^*$  produced from the output of algorithm 3 (after a suitable burnin) we can simulate  $s^* \sim p_N(s|\theta^*)$ . Then following the same reasoning as above, we have that  $s^*$  is a sample from  $p_N(s^*|s)$ , except that in this case it is easy to perform the sampling since  $p_N(s|\theta^*)$  is Gaussian by assumption. Therefore, here we have the (perhaps minor) incompatibility of using samples  $\theta^*$  generated using the BSL methodology (employing the unbiased likelihood estimator  $\hat{p}(s|\theta)$  in equation (10)) while the sampling of  $s^*$  uses the biased likelihood  $p_N(s|\theta)$ .

#### Additional posterior predictive checks for section 5.2.1

Here we consider further plots for posterior predictive checks (PPC) produced when using BSL on group 3, see section 5.2.1 in the manuscript. There we have reported the PPC for inter-subjects variability (Figure 7 in the manuscript) and the individual intra-subject variability pertaining to subject 1. Here we report further plots for intra-subject variability for two additional subjects, namely subject 2 and 3. See Figures 11–12, showing that the observed summaries are plausible according to the estimated model. Also in this case, most observed summaries are consistent with those produced by the prior predictive distribution.

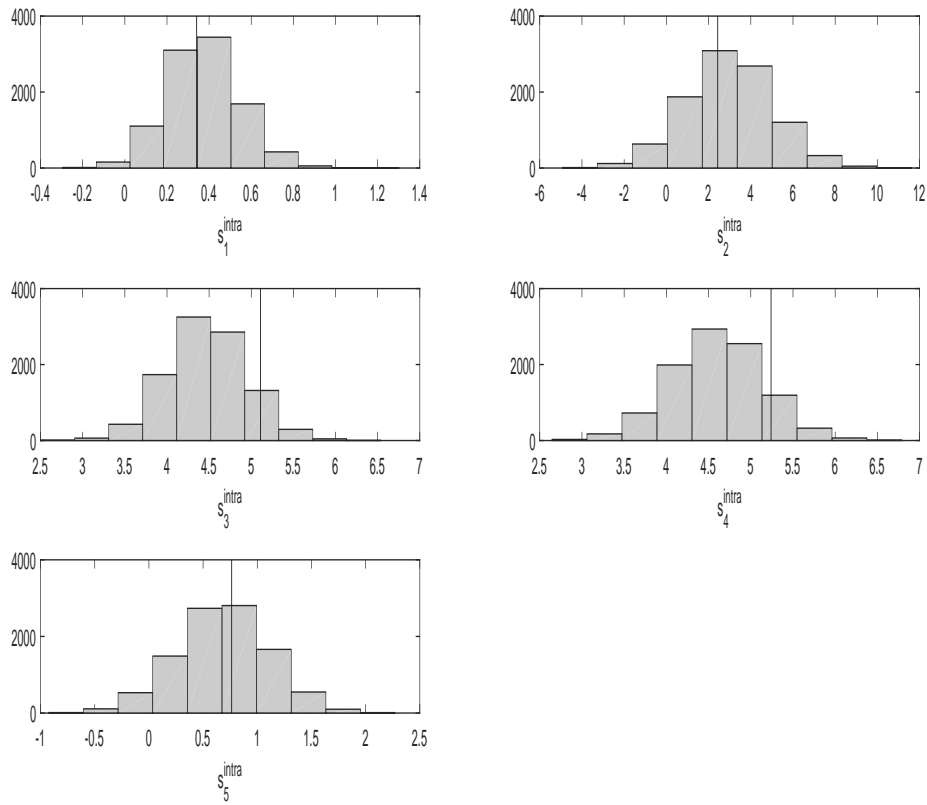


Figure 11: Posterior predictive checks for group 3 using the BSL parameter estimates. Distribution of the simulated statistics for the intra-subjects variability for subject 2:  $s_1^{\text{intra}}$  and  $s_2^{\text{intra}}$  (top),  $s_3^{\text{intra}}$  and  $s_4^{\text{intra}}$  (middle) and  $s_5^{\text{intra}}$  (bottom). Vertical lines mark the values for the corresponding statistics from the observed data.

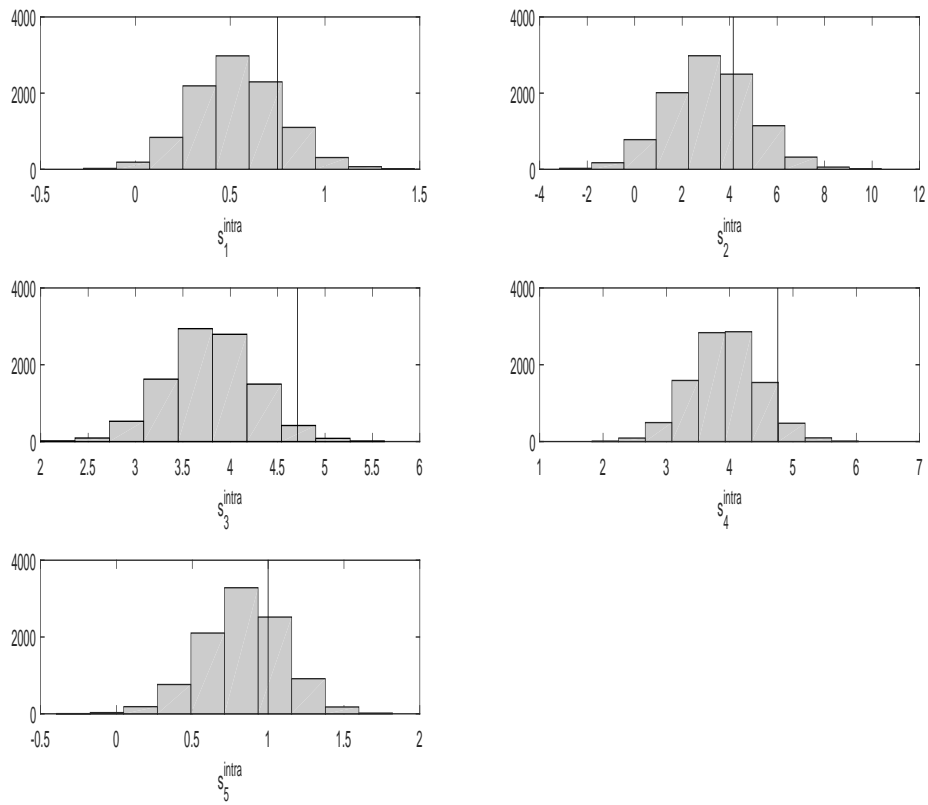


Figure 12: Posterior predictive checks for group 3 using the BSL parameter estimates. Distribution of the simulated statistics for the intra-subjects variability for subject 3:  $s_1^{\text{intra}}$  and  $s_2^{\text{intra}}$  (top),  $s_3^{\text{intra}}$  and  $s_4^{\text{intra}}$  (middle) and  $s_5^{\text{intra}}$  (bottom). Vertical lines mark the values for the corresponding statistics from the observed data.

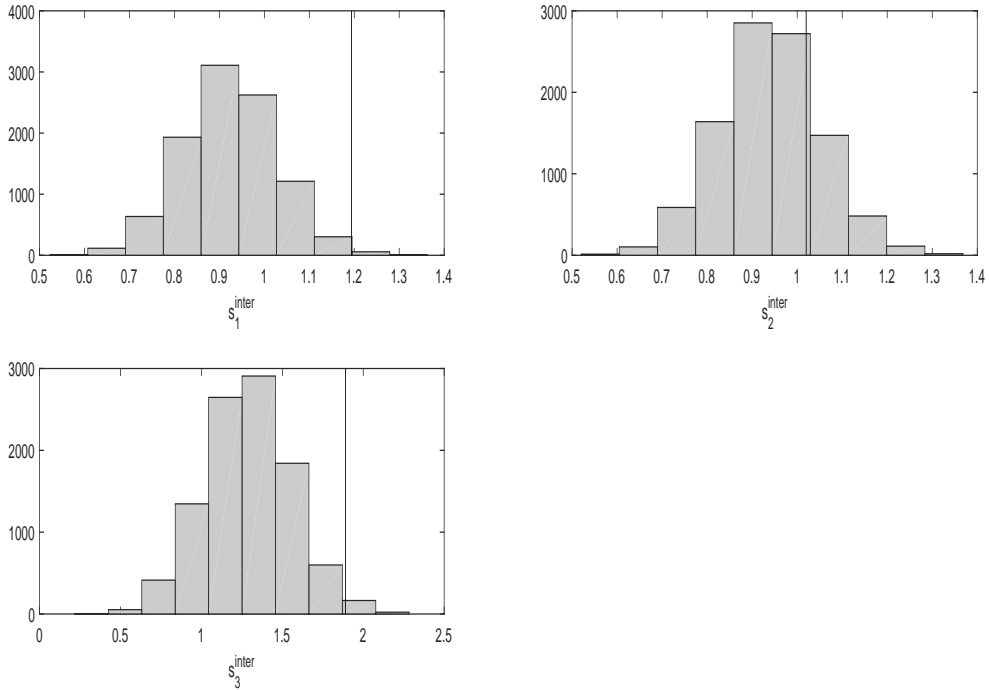


Figure 13: Posterior predictive checks for simulated data  $\mathcal{D}_2$  using the BSL parameter estimates. Distribution of the simulated statistics for the inter-subjects variability:  $s_1^{\text{inter}}$  (top left),  $s_2^{\text{inter}}$  (top right) and  $s_3^{\text{inter}}$  (bottom). Vertical lines mark the values for the corresponding statistics from the observed data.

### Posterior predictive checks for section 6.1

Here we enhance results obtained in section 6.1, pertaining the simulated data set  $\mathcal{D}_2$  having  $M = 17$  subjects. The inter-subjects features are in Figure 13. Intra-subject features for subject 1 are in Figure 14.

### Wider priors for section 5.2

Here we report results obtained by running BSL as in section 5.2, except for considering less informative priors for  $\log \bar{\delta}$ ,  $\sigma_\beta$  and  $\sigma_\delta$ , namely here we used  $\log \bar{\delta} \sim \mathcal{N}(0.7, 1.5^2)$ ,  $\sigma_\beta \sim \text{InvGam}(1, 0.5)$ ,  $\sigma_\delta \sim \text{InvGam}(1, 0.5)$ . All remaining priors are the same as in section 5.2. This way most of the prior mass for  $\log \bar{\delta}$  is contained in  $[-4, 4]$  (vs  $[-1.5, 1.5]$  in Figure 2 of the main article), and for  $\sigma_\beta$  and  $\sigma_\delta$  most of the prior mass is in  $(0, 4]$  (vs  $(0, 2]$  in Figure 2). Results are in Figure 15. By comparing with Figure 2 in the main article, we can tell that both  $\sigma_\beta$  and  $\sigma_\delta$  to some extent follow their priors (similarly to Figure 2), that is the available amount of data do not seem to contain enough information to allow estimation of these parameters. Regarding the posterior for the (log-)elimination rate  $\log \bar{\delta}$ , we notice a major shift towards smaller values (as compared to the counterpart in Figure 2) however the spread of the posterior has also increased. It seems that also this parameter is sensitive to its prior, at least in the small sample scenario.

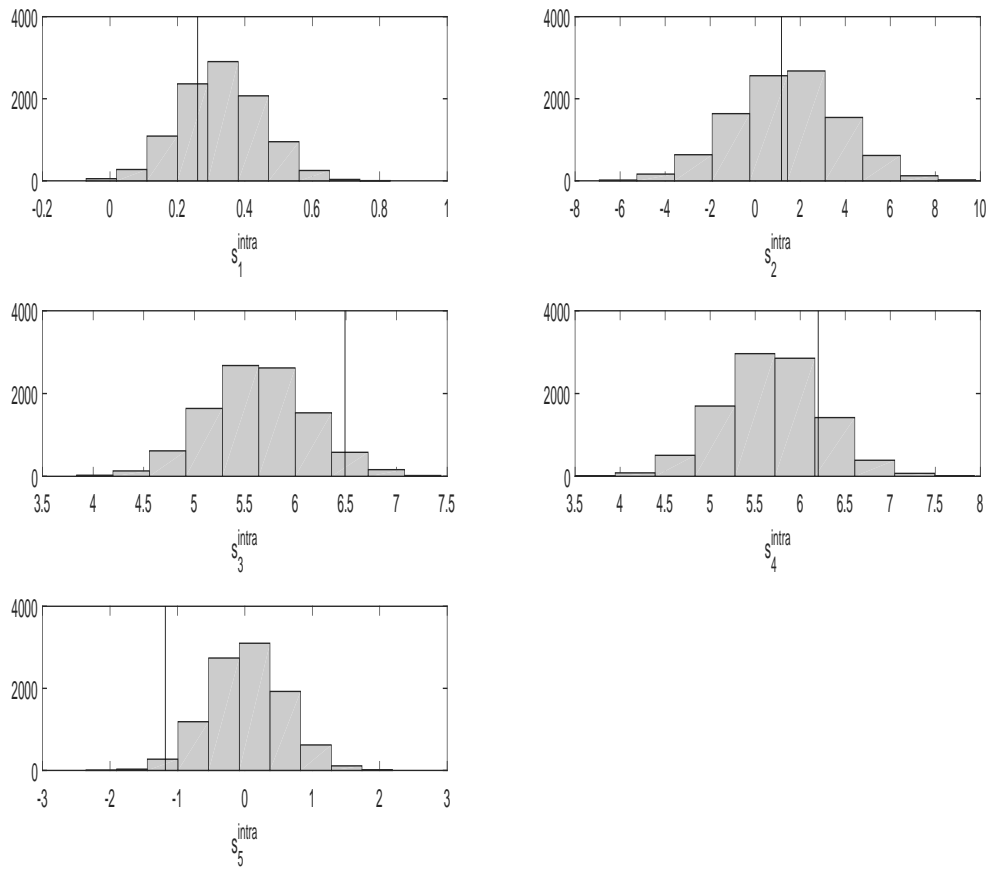


Figure 14: Posterior predictive checks for simulated data  $\mathcal{D}_2$  using the BSL parameter estimates. Distribution of the simulated statistics for the intra-subjects variability for subject 1:  $s_1^{\text{intra}}$  and  $s_2^{\text{intra}}$  (top),  $s_3^{\text{intra}}$  and  $s_4^{\text{intra}}$  (middle) and  $s_5^{\text{intra}}$  (bottom). Vertical lines mark the values for the corresponding statistics from the observed data.

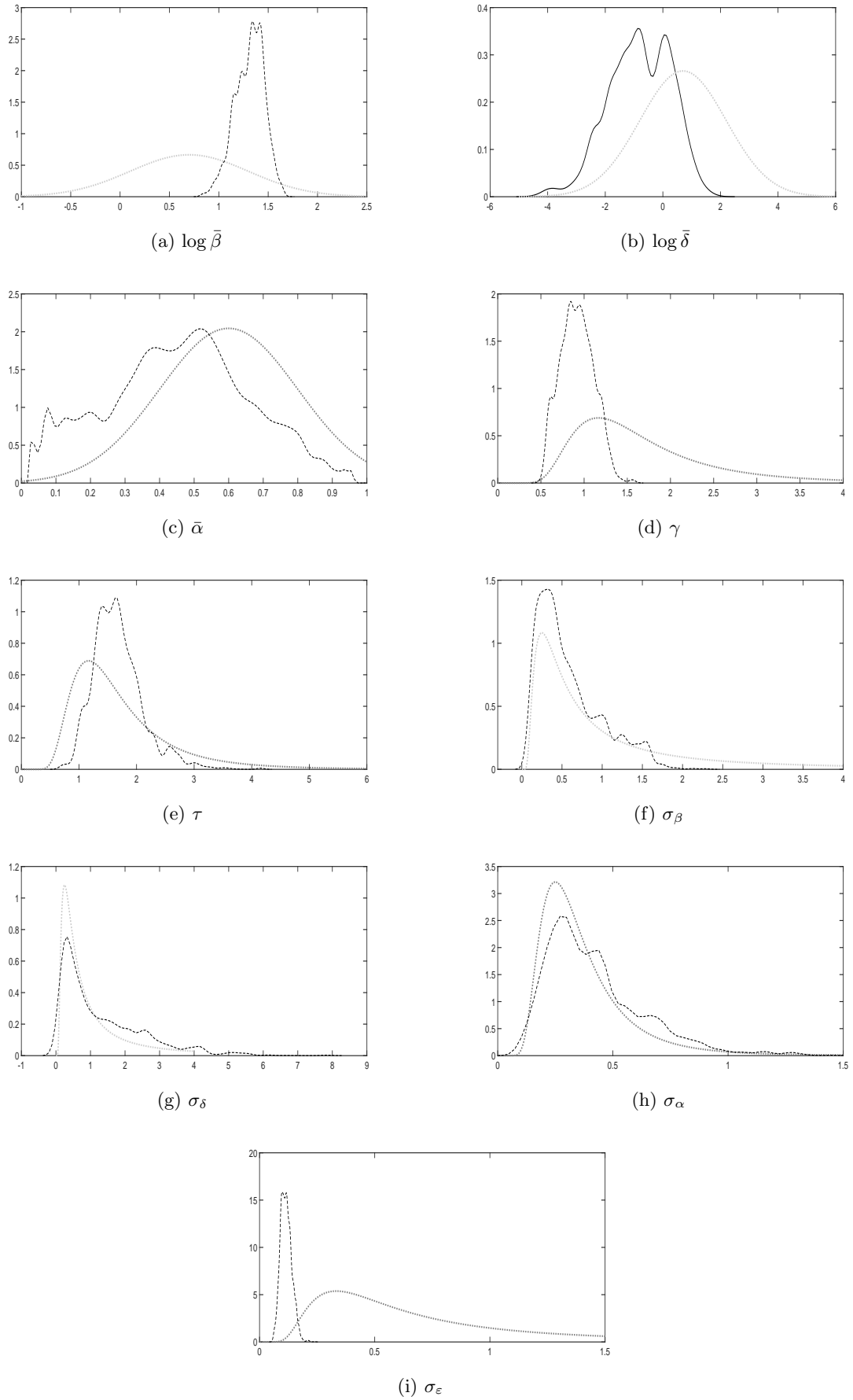


Figure 15: Treatment group 3 using less informative priors for  $\log \bar{\delta}$ ,  $\sigma_{\beta}$  and  $\sigma_{\delta}$ . Marginal posteriors obtained with synthetic likelihoods (dashed) and prior densities (dotted gray).